

Reciprocity in Directed Hypergraphs: Measures, Findings, and Generators

Sunwoo Kim^{*1}, Minyoung Choe^{†1}, Jaemin Yoo^{‡3}, and Kijung Shin^{§1,2}

¹Kim Jaechul Graduate School of AI, KAIST

²School of Electrical Engineering, KAIST

³Heinz College of Information Systems and Public Policy, Carnegie Mellon University

Abstract

Group interactions are prevalent in a variety of areas. Many of them, including email exchanges, chemical reactions, and bitcoin transactions, are directional, and thus they are naturally modeled as directed hypergraphs, where each hyperarc consists of the set of source nodes and the set of destination nodes. For directed graphs, which are a special case of directed hypergraphs, reciprocity has played a key role as a fundamental graph statistic in revealing organizing principles of graphs and in solving graph learning tasks. For general directed hypergraphs, however, even no systematic measure of reciprocity has been developed.

In this work, we investigate the reciprocity of 11 real-world hypergraphs. To this end, we first introduce eight axioms that any reasonable measure of reciprocity should satisfy. Second, we propose HYPERREC, a family of principled measures of hypergraph reciprocity that satisfy all the axioms. Third, we develop FASTHYPERREC, a fast and exact algorithm for computing the measures. Fourth, using them, we examine 11 real-world hypergraphs and discover patterns that distinguish them from random hypergraphs. Lastly, we propose REDi, an intuitive generative model for directed hypergraphs exhibiting the patterns.

1 Introduction

Beyond pairwise interactions, understanding and modeling group-wise interactions in complex systems have recently received considerable attention [Benson et al., 2018a, Comrie and Kleinberg, 2021, Do et al., 2020, Kook et al., 2020, Lee et al., 2021]. A *hypergraph*, which is a generalization of a graph, has been used widely as an appropriate abstraction for such group-wise interactions. Each hyperedge in a hypergraph is a set of any number of nodes, and thus it naturally represents a group-wise interaction.

Many group-wise interactions are directional, and they are modeled as a *directed hypergraph*, where each hyperarc consists of the set of source nodes and the set of destination nodes. Examples of directional group-wise interactions include email exchanges (from senders to receivers), chemical reactions [Yadati et al., 2020], road networks [Luo et al., 2022], and bitcoin transactions [Ranshous et al., 2017]; and they are modeled as directed hypergraphs for various applications, including metabolic-behavior prediction [Yadati et al., 2020] and traffic prediction [Luo et al., 2022]. See Figure 1 for an example of hypergraph modeling.

Reciprocity [Newman et al., 2002, Garlaschelli and Loffredo, 2004], which quantifies how mutually nodes are linked, has been used widely as a basic statistic of directed graphs, which are a special case of directed hypergraphs where every arc has exactly one source node and one destination node. Reciprocity increase understanding of a graph, especially potential organizing principles of it, and has proved useful for various tasks, including trust prediction [Nguyen et al., 2010], persistence prediction [Hidalgo and Rodríguez-Sickert, 2008], anomaly detection [Akoglu et al., 2012], and analysis of the spread of a computer virus through emails [Newman et al., 2002].

*kswoo97@kaist.ac.kr

†minyoung.choe@kaist.ac.kr

‡jaeminyoo@cmu.edu

§kijungs@kaist.ac.kr

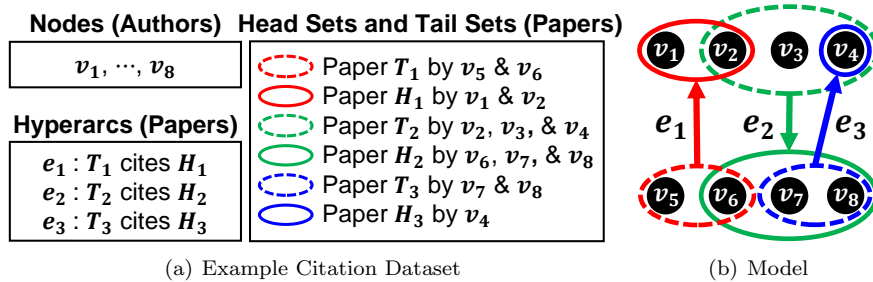


Figure 1: A citation dataset modeled as a directed hypergraph with 8 nodes and 3 hyperarcs. Nodes correspond to authors. Hyperarcs correspond to citations. The head set and tail set of each hyperarc correspond to sets of papers.

However, reciprocity has remained unexplored for directed hypergraphs, and to the best of our knowledge, no principled measure of reciprocity has been defined for directed hypergraphs. One straightforward approach is to first convert a directed hypergraph into an ordinary directed graph via clique expansion and then calculate standard reciprocity on the ordinary graph, as suggested in [Pearcy et al., 2014]. However, clique expansion may incur considerable information loss [Yadati et al., 2020, Dong et al., 2020, Yoon et al., 2020]. Thus, multiple directed hypergraphs whose reciprocity should differ, if they are determined by a proper measure, may become indistinguishable after being clique-expanded.

In this work, we investigate the reciprocity of real-world hypergraphs based on the first principled notion of reciprocity for directed hypergraphs. Our contributions toward this goal are summarized as follows:¹

- **Principled Reciprocity Measure:** We design HYPERREC, a family of probabilistic measures of hypergraph reciprocity. We prove that HYPERREC satisfy eight axioms that any reasonable measure of hypergraph reciprocity should satisfy, while baseline measures do not.
- **Fast and Exact Search Algorithm:** The size of search space for computing HYPERREC is exponential in the number of hyperarcs. We develop FASTHYPERREC, a fast and exact algorithm for computing HYPERREC.
- **Observations in Real-world Hypergraphs:** Using HYPERREC and FASTHYPERREC, we investigate 11 real-world directed hypergraphs, and discover three reciprocal patterns pervasive in them, which are verified using a null hypergraph model.
- **Realistic Generative Model:** To confirm our understanding of the patterns, we develop REDI, a directed-hypergraph generator based on simple mechanisms on individual nodes. Our experiments demonstrate that REDI yields directed hypergraphs with realistic reciprocal patterns.

For **reproducibility**, the code and data are available at <https://github.com/kswoo97/hyprec>.

In Section 2, we discuss preliminaries and related work. In Section 3, we propose a family of measures of hypergraph reciprocity with a computation algorithm. In Section 4, we discuss reciprocal patterns of real-world directed hypergraphs. In Section 5, we propose a generative model for directed hypergraphs. Lastly, we offer a conclusion in Section 6.

¹This work is an extended version of [Kim et al., 2022], which was presented at the 22nd IEEE International Conference on Data Mining (ICDM 2022). In the extended version, we introduce several theoretical extensions: (a) generalized versions of the axioms in Section 3.1 and a proof of Theorem 1 for the generalized versions (Appendix A), (b) seven baseline hypergraph reciprocity measures (Section 3.3), (c) a proof that none of the baseline measures satisfies all the axioms (Appendix B), and (d) proofs of Theorem 2 and Corollary 1 (Appendix A). In addition, we conduct additional experiments regarding (a) the efficiency of FASTHYPERREC (Figure 4 and Table 3 in Section 3.4), (b) the statistical significance of Observation 1 (Table 8 in Section 4.2), (c) the robustness of HYPERREC with respect to the choice of α (Tables 6 and 9 in Section 4.2), and (d) the verification of Observation 2 in 12 more real and synthetic hypergraphs (Figure 5 in 4.2 and Figure 7 in Section 5.2). At last, we provide one additional reciprocal pattern in real-world hypergraph (Observation 3: Figure 6 in Section 4.2) and verify whether REDI can reproduce this pattern.

Table 1: Frequently-used symbols.

Notation	Definition
$G = (V, E)$	hypergraph with nodes V and hyperarcs E
$e_i = \langle H_i, T_i \rangle$	hyperarc (or a target arc)
H_i, T_i	head set and tail set of a hyperarc e_i
$R_i = \{e'_1, \dots, e'_{ R_i }\}$	reciprocal set of a hyperarc e_i (see Section 3.1 for details)
$r(e_i, R_i)$	reciprocity of a target arc e_i with a reciprocal set R_i
$r(G)$	reciprocity of a hypergraph G
$d_{in}(v), d_{out}(v)$	in-degree and out-degree of a node v
$ A $	cardinality of a set A (i.e., number of elements in A)

2 Basic Concepts and Related Work

In this section, we introduce some basic concepts and review related studies. See Table 1 for frequently-used symbols.

2.1 Basic Concepts

A *directed hypergraph* $G = (V, E)$ consists of a set of nodes $V = \{v_1, \dots, v_{|V|}\}$ and a set of *hyperarcs* $E = \{e_1, \dots, e_{|E|}\} \subseteq \{\langle H, T \rangle : H \subseteq V, T \subseteq V\}$. For each hyperarc $e_i = \langle H_i, T_i \rangle \in E$, H_i indicates the *head set* and T_i indicates the *tail set*. In Figure 1, the hyperarc $e_1 = \langle H_1, T_1 \rangle \in E$ is represented as an arrow that heads to $H_1 = \{v_1, v_2\}$ from $T_1 = \{v_5, v_6\}$. It is assumed typically and also in this work that, in every hyperarc, the head set and the tail set are disjoint (i.e., $H_i \cap T_i = \emptyset, \forall i = 1, \dots, |E|$). The *in-degree* $d_{in}(v) = |\{e_i \in E : v \in H_i\}|$ of a node $v \in V$ is the number of hyperarcs that include v as a head. Similarly, the *out-degree* $d_{out}(v) = |\{e_i \in E : v \in T_i\}|$ of $v \in V$ is the number of hyperarcs that include v as a tail.

From now on, we will use the term *hypergraph* to indicate a *directed hypergraph* and use the term *undirected hypergraph* to indicate an undirected one. We will also use the term *arc* to indicate a hyperarc when there is no ambiguity.

2.2 Related Work

Reciprocity of Directed Graphs: Reciprocity of directed graphs (i.e., a special case of directed hypergraphs where all head sets and tail sets are of size one) is a tendency of two nodes to be mutually linked [Newman et al., 2002, Garlaschelli and Loffredo, 2004]. This is formally defined as $|E^{\leftrightarrow}|/|E|$, where $|E|$ is the number of edges in a graph, and $|E^{\leftrightarrow}|$ is the number of edges whose opposite directional arc exists, i.e., $e = \langle \{v_i\}, \{v_j\} \rangle \in E^{\leftrightarrow}$ if and only if $\langle \{v_j\}, \{v_i\} \rangle \in E$. The notion was extended to weighted graphs [Squartini et al., 2013, Akoglu et al., 2012], and using them, the relationship between degree and reciprocity was investigated [Akoglu et al., 2012]. Moreover, the preferential attachment model [Albert and Barabási, 2002] was extended by adding a parameter that controls the probability of creating a reciprocal edge for generating reciprocal graphs [Cirkovic et al., 2022, Wang and Resnick, 2022]. Refer to Section 1 for more applications of reciprocity.

Patterns and Generative Models of Hypergraphs: Hypergraphs have been used widely for modeling group-wise interactions in complex systems, and considerable attention has been paid to the structural properties of real-world hypergraphs, with focuses on node degrees [Do et al., 2020, Kook et al., 2020], singular values [Do et al., 2020, Kook et al., 2020], diameter [Do et al., 2020, Kook et al., 2020], density [Kook et al., 2020], core structures [Bu et al., 2023], the occurrences of motifs [Lee et al., 2020, Lee and Shin, 2021], simplicial closure [Benson et al., 2018a], ego-networks [Comrie and Kleinberg, 2021], the repetition of hyperedges [Benson et al., 2018b, Choo and Shin, 2022], and the overlap of hyperedges [Lee et al., 2021]. Many of these patterns can be reproduced by hypergraph generative models that are based on intuitive mechanisms [Benson et al., 2018b, Do et al., 2020, Kook et al., 2020, Lee et al., 2021]. Such models can be used for anonymization and graph upscaling in addition to testing our understanding of the patterns [Leskovec, 2008]. All the above studies are limited to undirected hypergraphs, while this paper focuses on directed hypergraphs.

Directed Hypergraphs and Reciprocity: Directed hypergraphs have been used for modeling chemical reactions [Yadati et al., 2020], knowledge bases [Yadati et al., 2021], road networks [Luo et al., 2022], bitcoin transactions [Ranshous et al., 2017], etc. To the best of our knowledge, there has been only one attempt to measure the reciprocity of directed hypergraphs [Pearcy et al., 2014], where (a) a hypergraph G is transformed into a weighted digraph \bar{G} by *clique expansion*, i.e., by replacing each arc $e_i = \langle H_i, T_i \rangle$ with the bi-clique from T_i to H_i , (b) a weighted digraph \bar{G}' is obtained in the same way from a hypergraph G' where, the perfectly reciprocal arc $\langle T_i, H_i \rangle$ of each arc $e_i = \langle H_i, T_i \rangle \in E$ is added if it is not already in E , and (c) $tr(\bar{A}^2)/tr(\bar{A}'^2)$, where \bar{A} and \bar{A}' are the weighted adjacency matrices of \bar{G} and \bar{G}' , respectively, is computed as the reciprocity of G . Note that $tr(\bar{A}^2)$ corresponds to the weighted count of paths of length two in \bar{G} that start and end at the same node, which is the same as the weighted count of mutually linked pairs of nodes in \bar{G} , and $tr(\bar{A}'^2)$ is the count in the perfectly reciprocal counterpart. However, as discussed in Section 1, clique expansion may cause substantial information loss [Yadati et al., 2020, Dong et al., 2020, Yoon et al., 2020], and thus multiple directed hypergraphs whose reciprocities should differ, if they are determined by a proper measure, can be transformed into the same directed graphs by clique expansion. We further analyze the limitations of this approach based on axioms in the following section.

3 Directed Hypergraph Reciprocity

In this section, we present eight necessary properties of an appropriate hypergraph reciprocity measure. Then, we present a family of reciprocity measures, namely HYPERREC, and an algorithm for fast computation of them. Lastly, we compare HYPERREC with baseline measures to support its soundness.

3.1 Framework and Axioms

We present our framework for measuring hypergraph reciprocity. Then, we suggest eight axioms that any reasonable reciprocity measure must satisfy.

Framework for Hypergraph Reciprocity: Given a hypergraph G , we measure its reciprocity at two levels:

- How much each arc (i.e., group interaction) is reciprocal.
- How much the entire hypergraph G is reciprocal.

For a *target arc*, which we measure reciprocity for, multiple arcs should be involved in measuring its reciprocity inevitably. For example, in Figure 1, arc e_2 's head set and tail set overlap with e_1 and e_3 's tail set and head set, respectively, and thus we should consider both e_1 and e_3 in measuring e_2 's reciprocity. In graphs, however, only the arc with the opposite direction is involved in the reciprocity of an arc. This unique characteristic of hypergraphs poses challenges in measuring reciprocity. The *reciprocal set* R_i of a target arc e_i is the set of *reciprocal arcs* that we use to compute the reciprocity of e_i . We use $r(e_i, R_i)$ to denote the *reciprocity of an arc* e_i , where the domain is $E \times 2^E$.² In graphs, a traditional reciprocity measure [Newman et al., 2002] is defined as the proportion of arcs between nodes that point both ways, and if we assign 1 to such an arc and 0 to the others as reciprocity, the proportion is equivalent to the average reciprocity of arcs. Similarly, we regard, as the *reciprocity of a hypergraph* G , the average reciprocity of arcs, i.e.,

$$r(G) := \frac{1}{|E|} \sum_{i=1}^{|E|} r(e_i, R_i). \quad (1)$$

Motivations of axioms: What are the characteristics required for $r(e_i, R_i)$ and $r(G)$? We introduce eight axioms that any reasonable measure of $r(e_i, R_i)$ (**Axioms** 1-5) and $r(G)$ (**Axioms** 6-8) should satisfy. We first provide the motivation and necessity of the proposed axioms.

- **Incremental changes:** Understanding when a value of a measure increases (decreases) helps users to understand how the measure works and have faith in the values the measure returns. Without this understanding, one cannot trust the measure, and this unreliability towards a measure may lead to misinterpretation of the measured value. Thus, we propose **Axioms** 1-4 (and their generalized axioms) to describe the cases where the value of a reciprocity measure increases (decreases).
- **Boundness:** Establishing a finite range for a measure helps an intuitive comprehension of the numerical extent of a characteristic. For instance, if a measure does not lie in a fixed range, it becomes challenging to readily ascertain whether a particular hypergraph is reciprocal or not. Furthermore, a measure with

²Note that all arcs in R_i are used in computing the reciprocity of e_i , and thus it does not correspond to a search space.

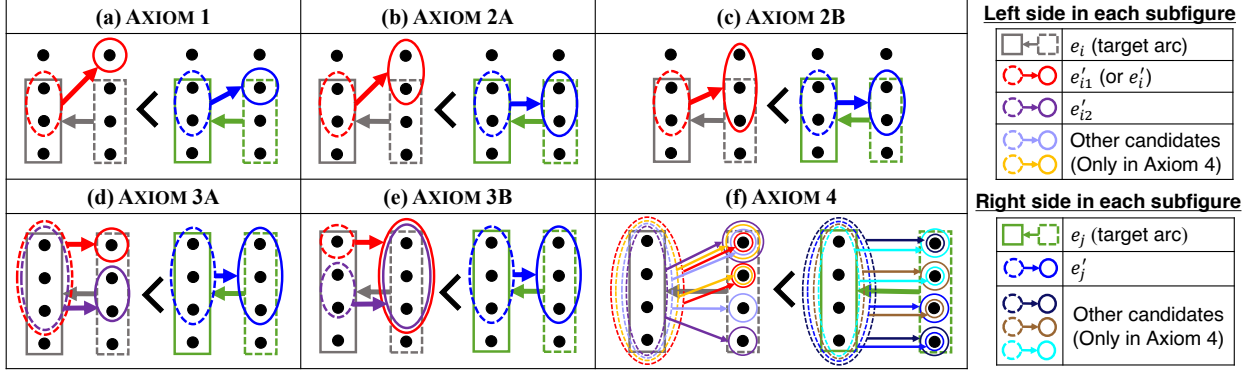


Figure 2: Examples for **Axioms** 1-4. In each subfigure, the reciprocity of the arc e_i on the left side should be smaller than that of the arc e_j on the right side. This inequality holds by HYPERREC (see Section 3.2) in all subfigures. Specifically, if $\alpha = 1$, $r(e_i)$ & $r(e_j)$ are 0.0000 & 0.3605 in (a), 0.2697 & 0.5394 in (b), 0.4444 & 0.5394 in (c), 0.3167 & 0.6466 in (d), 0.3233 & 0.6466 in (e), and 0.2347 & 0.2500 in (f).

a defined finite range enhances the ability to make meaningful comparisons across diverse hypergraphs. Motivated by this intuition, we propose **Axiom 5** and **Axiom 7**, which suggest the bound of hyperarc and hypergraph reciprocity measures, respectively.

- **Reducibility:** Reciprocity in an ordinary directed graph is a well-known statistic that is widely used in various fields of study [Nguyen et al., 2010, Hidalgo and Rodríguez-Sickert, 2008, Newman et al., 2002] (see Section 1 for details). Since a directed hypergraph is a generalization of an ordinary directed graph, one would expect that a directed hypergraph reciprocity measure should be equivalent to the common directed graph reciprocity when applied to any hypergraph containing only hypercars with head sets and tail sets of size 1 (i.e., directed graph. where $|H_i| = |T_i| = 1, \forall (H_i, T_i) \in E$). Thus, we propose **Axiom 6**, which suggests this characteristic
- **Reachability:** Identifying whether the upper bound of a measure is truly achievable or not plays a crucial role in ensuring the reliability of the measure’s range and the accurate interpretability of its returned value. For example, let’s consider a reciprocity measure with a known upper bound of 1, but it can actually only reach the value of 0.2. In this scenario, if a particular hypergraph achieves the reciprocity value of 0.2, which is actually the maximum possible value for a hypergraph, one may think the corresponding hypergraph is not highly reciprocal, since the known upper bound of 1. Thus, we propose **Axiom 8** to formalize the reachability of the maximum reciprocity value.

Details of axioms: In **Axioms** 1-4, we compare the reciprocity of two target arcs e_i and e_j whose reciprocal sets are R_i and R_j , respectively. Moreover, in **Axiom** 2-4, we commonly assume two target arcs e_i and e_j are of equal size (i.e., $|H_i| = |H_j|$ and $|T_i| = |T_j|$). Here, we say two arcs e_i and $e_k \in R_i$ **inversely overlap** if and only if $H_i \cap T_k \neq \emptyset$ and $T_i \cap H_k \neq \emptyset$. Below, the statements in **Axioms** 1-4 are limited to the examples in Figure 2 for simplicity. Each statement of **Axioms** 1-4 is generalized in **Generalized Axioms** 1-4.

Axiom 1 (Existence of Inverse Overlap). *In Figure 2(a), $r(e_i, R_i) < r(e_j, R_j)$ should hold. Roughly, an arc with at least one inverse-overlapping reciprocal arc is more reciprocal than an arc with no inverse-overlapping reciprocal arcs.*

Generalized Axiom 1 (Existence of Inverse Overlap). *Consider two arcs e_i and e_j . If R_i and R_j satisfy*

$$\begin{aligned} (i) \quad & \forall e'_i \in R_i : \min(|H_i \cap T'_i|, |T_i \cap H'_i|) = 0, \\ (ii) \quad & \exists e'_j \in R_j : \min(|H_j \cap T'_j|, |T_j \cap H'_j|) \geq 1, \end{aligned}$$

then the following inequality holds:

$$r(e_i, R_i) < r(e_j, R_j).$$

Axiom 2 (Degree of Inverse Overlap). *In Figures 2(b-c), $r(e_i, R_i) < r(e_j, R_j)$ should hold. Roughly, an arc that inversely overlaps with reciprocal arcs to a greater extent (with a larger intersection and/or with a smaller difference, which are considered separately in the generalized axioms) is more reciprocal.*

Generalized Axiom 2A (Degree of Inverse Overlap: More Overlap). Consider two arcs e_i and e_j of the same size (i.e., $(|H_i| = |H_j|) \wedge (|T_i| = |T_j|)$). If $R_i = \{e'_i\}$ and $R_j = \{e'_j\}$ satisfy

$$\begin{aligned} & |H'_i| = |H'_j|, \quad |T'_i| = |T'_j|, \quad \text{and} \\ (i) \quad & 0 < |H'_i \cap T_i| < |H'_j \cap T_j| \quad \text{and} \quad 0 < |T'_i \cap H_i| \leq |T'_j \cap H_j| \quad \text{or} \\ (ii) \quad & 0 < |H'_i \cap T_i| \leq |H'_j \cap T_j| \quad \text{and} \quad 0 < |T'_i \cap H_i| < |T'_j \cap H_j|, \end{aligned}$$

then the following inequality holds:

$$r(e_i, R_i) < r(e_j, R_j).$$

Generalized Axiom 2B (Degree of Inverse Overlap: Small Difference). Consider two arcs e_i and e_j of the same size (i.e., $(|H_i| = |H_j|) \wedge (|T_i| = |T_j|)$). If $R_i = \{e'_i\}$ and $R_j = \{e'_j\}$ satisfy

$$|H'_i| > |H'_j|, \quad |T'_i| = |T'_j|, \quad 0 < |H'_i \cap T_i| = |H'_j \cap T_j|, \quad \text{and} \quad 0 < |T'_i \cap H_i| = |T'_j \cap H_j|,$$

then the following inequality should hold:

$$r(e_i, R_i) < r(e_j, R_j).$$

Axiom 3 (Number of Reciprocal Arcs). In Figures 2(d-e), $r(e_i, R_i) < r(e_j, R_j)$ should hold. Roughly, when two arcs inversely overlap equally with their reciprocal sets, an arc with a single reciprocal arc is more reciprocal than one with multiple reciprocal arcs.

Below, we generalize **Axiom 3** by dividing it into two cases. Although the below two statements compare an arc with a single reciprocal arc and an arc with exactly two reciprocal arcs, these statements can be further extended to encompass a comparison of the former and an arc with two or more reciprocal arcs. These extended statements remain valid for our proposed measure (refer to **Remark 1** in Appendix A).

Generalized Axiom 3A (Number of Reciprocal Arcs Differs: Identical Tail Sets). Let $e'_k \subseteq_{(R)} e_k$ indicate $H'_k \subseteq T_k$ and $T'_k \subseteq H_k$. Consider two arcs e_i and e_j of the same size (i.e., $(|H_i| = |H_j|) \wedge (|T_i| = |T_j|)$). If $R_i = \{e'_{i1}, e'_{i2}\}$ and $R_j = \{e'_j\}$ satisfy

$$\begin{aligned} e'_{i1} \subseteq_{(R)} e_i, \quad e'_{i2} \subseteq_{(R)} e_i, \quad e'_j \subseteq_{(R)} e_j, \quad T'_{i1} = T'_{i2}, \quad |T'_{i1}| = |T_j|, \\ H'_{i1} \cap H'_{i2} = \emptyset, \quad \text{and} \quad |(H'_{i1} \cup H'_{i2}) \cap T_i| = |H'_j \cap T_j|, \end{aligned}$$

then the following inequality should hold:

$$r(e_i, R_i) < r(e_j, R_j).$$

Generalized Axiom 3B (Number of Reciprocal Arcs: Identical Head Sets). Let $e'_k \subseteq_{(R)} e_k$ indicate $H'_k \subseteq T_k$ and $T'_k \subseteq H_k$. Consider two arcs e_i and e_j of the same size (i.e., $(|H_i| = |H_j|) \wedge (|T_i| = |T_j|)$). If $R_i = \{e'_{i1}, e'_{i2}\}$ and $R_j = \{e'_j\}$ satisfy

$$\begin{aligned} e'_{i1} \subseteq_{(R)} e_i, \quad e'_{i2} \subseteq_{(R)} e_i, \quad e'_j \subseteq_{(R)} e_j, \quad H'_{i1} = H'_{i2}, \quad |H'_{i1}| = |H_j|, \\ T'_{i1} \cap T'_{i2} = \emptyset, \quad \text{and} \quad |(T'_{i1} \cup T'_{i2}) \cap H_i| = |T'_j \cap H_j|, \end{aligned}$$

then the following inequality should hold:

$$r(e_i, R_i) < r(e_j, R_j).$$

Axiom 4 (Bias). In Figure 2(f), $r(e_i, R_i) < r(e_j, R_j)$ should hold. Roughly, when two arcs inversely overlap **equally** with their reciprocal sets, an arc whose reciprocal arcs are equally reciprocal to all nodes in the arc is more reciprocal than one with reciprocal arcs **biased** towards a subset of nodes in the arc.

Generalized Axiom 4 (Bias). Consider two arcs e_i and e_j of the same size (i.e., $(|H_i| = |H_j|) \wedge (|T_i| = |T_j|)$). If R_i and R_j satisfy

- (i) $|R_i| = |R_j| = |T_i| = |T_j|$, and $|T'_i| = |T'_j|$, $\forall e'_i \in R_i$, $\forall e'_j \in R_j$,
- (ii) $T'_i = H_i$, $H'_i \subset T_i$, and $|H'_i| = 2$, $\forall e'_i \in R_i$,
- (iii) $T'_j = H_j$, $H'_j \subset T_j$, and $|H'_j| = 2$, $\forall e'_j \in R_j$,
- (iv) $\exists u, v \in T_i$ where $|\{u \in H'_i \mid e'_i \in R_i\}| \neq |\{v \in H'_i \mid e'_i \in R_i\}|$ (2)
- (v) $\forall u, v \in T_j$ where $|\{u \in H'_j \mid e'_j \in R_j\}| = |\{v \in H'_j \mid e'_j \in R_j\}|$, (3)

then the following inequality should hold:

$$r(e_i, R_i) < r(e_j, R_j).$$

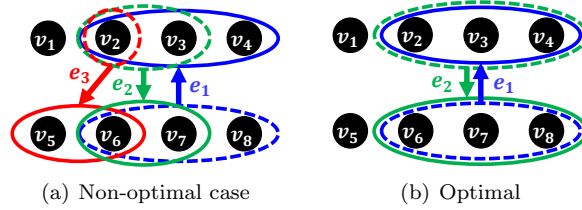


Figure 3: Examples for describing the computation of transition probabilities.

Axiom 5 (Upper and Lower Bounds). *The reciprocity of any arc should be within within a fixed finite range. Without loss of generality, we assume that the reciprocity values are within the range of $[0, 1]$, i.e., for every $e_i \in E$ and $R_i \in 2^E$, $r : E \times 2^E \mapsto [0, 1]$ should hold. Note that any fixed finite range can be re-scaled to $[0, 1]$.*

Now, we present the axioms defined at the hypergraph level.

Axiom 6 (Inclusion of Graph Reciprocity). *The graph reciprocity [Newman et al., 2002] should be included as a special case. That is, if G is a graph (i.e., $|H_i| = |T_i| = 1, \forall i \in \{1, \dots, |E|\}$), then the following equality should hold:*

$$r(G) = |E^{\leftrightarrow}|/|E|, \quad (4)$$

where E^{\leftrightarrow} is the set of arcs between nodes that point each other in both directions.

Axiom 7 (Upper and Lower Bounds). *The reciprocity of any hypergraph should be within a fixed finite range. Without loss of generality, we assume that the reciprocity values are within the range of $[0, 1]$, i.e., for any hypergraph G , the reciprocity function $r : G \mapsto [0, 1]$ should hold. Note that any fixed finite range can be re-scaled to $[0, 1]$.*

Axiom 8 (Reachability of Bounds). *The maximum reciprocity, which is 1 by **Axiom 7**, should be reachable from any hypergraph by adding specific arcs. That is, for every $G = (V, E)$, there exist $G^+ = (V, E^+)$ with $E^+ \supseteq E$ such that $r(G^+) = 1$. Similarly, the minimum reciprocity, which is 0 by **Axiom 7**, should be reachable from any hypergraph by removing specific arcs. That is, for every $G = (V, E)$, there exist $G^- = (V, E^-)$ with $E^- \subseteq E$ such that $r(G^-) = 0$.*

Note that **Axiom 8** is about whether the maximum and minimum values of a reciprocity measure are attainable or not (i.e., whether its bounds are tight or not), and it does not specify the situation when the value of a measure is maximized or minimized.

3.2 Proposed Measure of Hypergraph Reciprocity: HyperRec

We propose HYPERREC, a family of principled hypergraph-reciprocity measures based on transition probability.

Transition Probability: For a target arc $e_i = \langle H_i, T_i \rangle$ and its reciprocal arcs R_i , the **transition probability** $p_h(v)$ from a head set node $v_h \in H_i$ to each node v is the probability of a random walker transiting from v_h to v when she moves to a uniform random tail-set node of a uniform random arc among the reciprocal arcs incident to v_h . For example, consider a target arc e_1 and a reciprocal set $R_1 = \{e_2, e_3\}$ in Figure 3(a). For a head set node v_2 of the target arc, the reciprocal arcs incident to it are $\{e_2, e_3\}$. The node v_7 is only in the head set of e_2 , and thus the transition probability $p_2(v_7) = P(e_2 | \{e_2, e_3\}) \times P(v_7 | H_2) = 0.5 \times 0.5 = 0.25$. Similarly, since the node v_6 is in the head set of both e_2 and e_3 , $p_2(v_6) = P(e_2 | \{e_2, e_3\}) \times P(v_6 | H_2) + P(e_3 | \{e_2, e_3\}) \times P(v_6 | H_3) = 0.5 \times 0.5 + 0.5 \times 0.5 = 0.5$. Since, v_8 is not in tail set of any reciprocal arc, $p_2(v_8) = 0$. For a head set node v_3 of the target arc, the only reciprocal arc incident to it is e_2 . Since the node v_6 is in the head set of e_2 , $p_3(v_6) = P(e_2 | \{e_2\}) \times P(v_6 | T_2) = 1.0 \times 0.5 = 0.5$.

There might be some head set nodes that are not incident to any reciprocal arc. For example, v_4 in Figure 3(a) is such a node when the target arc is e_1 and the reciprocal set is $R_1 = \{e_2, e_3\}$. We assume that, from such a node, the random walker always transits to the virtual **sink node** $v_{sink} \notin V$.

Then, for each head set node $v_h \in H_i$ of a target arc e_i , a **transition probability distribution** over $V \cup \{v_{sink}\}$ is defined, and we use p_h to denote it. We also denote an **optimal transition probability distribution** by p_h^* , which is a transition probability distribution when the perfectly reciprocal arc

$e_i^* = \langle H_i^* = T_i, T_i^* = H_i \rangle$ is assumed as the reciprocal arc of e_i , i.e., $R_i = \{e_i^*\}$. For example, in Figure 3(b), e_2 is the perfectly reciprocal arc of e_1 . The following equality always holds:

$$p_h^*(v) = \begin{cases} \frac{1}{|T_i|} & \text{if } v \in T_i, \\ 0 & \text{otherwise.} \end{cases}$$

Proposed Measures: Based on the above concepts, we propose HYPERREC (Hypergraph Reciprocity) as a family of principled measures of hypergraph reciprocity. We notice that reciprocal arcs in a graph lead to paths of length two that start and end at the same node. Thus, intuitively, in a hypergraph, a target arc should become more reciprocal if its reciprocal arcs allow for heading back to the head-set nodes of the target arc more “accurately”. In order to measure numerically the accuracy for a target arc e_i , we compare the transition probability distribution p_h from each head-set node $v_h \in H_i$ with the optimal distribution p_h^* .

While any distance function \mathcal{L} can be used to quantify the difference between p_h and p_h^* , we use the *Jensen-Shannon Divergence* (JSD) [Lin, 1991] since it is a symmetric measure that can handle zero mass in both distributions. The JSD between distributions p and q with domain D is defined as

$$\mathcal{L}(p, q) := \sum_{i \in D} \left(\frac{p(i)}{2} \log \frac{2p(i)}{p(i) + q(i)} + \frac{q(i)}{2} \log \frac{2q(i)}{p(i) + q(i)} \right).$$

Based on \mathcal{L} , we define HYPERREC of an arc e_i whose reciprocal set is R_i as

$$r(e_i, R_i) := \left(\frac{1}{|R_i|} \right)^\alpha \left(1 - \frac{\sum_{v_h \in H_i} \mathcal{L}(p_h, p_h^*)}{|H_i| \cdot \mathcal{L}_{\max}} \right), \quad (5)$$

where $\alpha \in (0, 1]$ is a constant controlling the degree of penalization of a large reciprocal set, and \mathcal{L}_{\max} is the maximum value of the distance measure \mathcal{L} , which is $\log 2$ for the JSD. Note that the value of $r(e_i, R_i)$ becomes larger if $\mathcal{L}(p_h, p_h^*)$ becomes small, implying that an arc is more reciprocal if its transition distribution becomes closer to the optimal distribution.

Note that as the value of α increases, the penalty that occurs from the size of the reciprocal set (i.e., $|R_i|$) increases. This allows HYPERREC to effectively capture the user’s preferences regarding the impact of reciprocal set size on reciprocity. For instance, in certain domains, users may believe that, under the same conditions, an arc with a larger number of reciprocal arcs is considerably less reciprocal compared to an arc with fewer reciprocal arcs. To reflect this belief, a higher value of α can be set. However, in domains where the size of the reciprocal set is relatively less significant in relation to reciprocity, a smaller value of α can be employed. The flexibility of choosing α allows HYPERREC to adapt to different scenarios and user preferences.

Since the value of $r(e_i, R_i)$ varies depending on the specific choice of α , HYPERREC can be regarded as a family of hypergraph-reciprocity measures. Throughout the remainder of the paper, we use HYPERREC to denote any measure that falls within the HYPERREC family, unless explicitly mentioned otherwise.

Composing Reciprocal Sets: The value of $r(e_i, R_i)$ is dependent on how we select the reciprocal set R_i from the set E of all arcs. For each target arc e_i , we propose to choose non-empty $R_i \subseteq E$ that maximizes the reciprocity $r(e_i, R_i)$ of e_i , i.e.,

$$R_i := \operatorname{argmax}_{R_i' \subseteq E, R_i' \neq \emptyset} r(e_i, R_i'). \quad (6)$$

In summary, according to HYPERREC, the reciprocity of an arc $e_i \in E$ is

$$r(e_i) := \max_{R_i \subseteq E, R_i \neq \emptyset} r(e_i, R_i), \quad (7)$$

and by Eq. (1), the reciprocity of G is $r(G) := \frac{1}{|E|} \sum_{i=1}^{|E|} r(e_i)$.

Strengths of HyperRec: HYPERREC satisfies all proposed **Axioms** regardless of the value of $\alpha > 0$, as stated in Theorem 1, while none of the considered baseline measures, which are described below, does.

Theorem 1 (Soundness of HYPERREC). HYPERREC always satisfies **Axioms 1-8 and Generalized Axioms 1, 2A, 2B, 3A, 3B, and 4**

Proof. See the caption of Figure 2 for the numerical values for the examples. Full proofs can be found in Appendix A.2. \square

Note that while any distance function can be utilized as \mathcal{L} in Eq (5), the selected function should enable HYPERREC to satisfy all the axioms to ensure the soundness of HYPERREC.

Limitations of HyperRec: One limitation of HYPERREC is its high computational cost, as it involves finding maximum reciprocity value over $O(2^{|E|})$ potential reciprocal sets. This search, however, is necessary to satisfy the proposed axioms, as discussed in Section 3.3 In Section 3.4, we discuss methods to reduce the search space and thus mitigate this computational burden, without affecting the reciprocity value.

3.3 Baseline Approaches and Axiomatic Analysis

Below, we present the baseline measures considered in our work.

B1. Percy et al. [2014]: Refer to the last paragraph of Section 2 for details of this measure. This measure is defined only for the entire hypergraph. For the arc-level axioms (i.e., **Axioms 1-5**), we use the hypergraphs that consist only of arcs that are mentioned in each axiom. That is, we compare the reciprocity of $G_i = (V, \{e_i\} \cup R_i)$ and $G_j = (V, \{e_j\} \cup R_j)$.

B2. Ratio of Covered Pairs: This measures, roughly, how accurately pair interactions within a target arc are matched with those within reciprocal arcs. We define the pair interactions within e_i as:

$$K(e_i) = \{\langle v_h, v_t \rangle \mid v_h \in H_i, v_t \in T_i\}.$$

We also define the set of inverse pair-interactions for e_k as:

$$K^{-1}(e_k) = \{\langle v_t, v_h \rangle \mid v_h \in H_k, v_t \in T_k\}.$$

Then, inspired by the Jaccard Index, we define the measure as the ratio of identical members between $K(e_i)$ and $K^{-1}(e_k)$ for all $e_k \in R_i$ as follows:

$$r(e_i, R_i) = \frac{|K(e_i) \cap \bigcup_{e_k \in R_i} K^{-1}(e_k)|}{|K(e_i) \cup \bigcup_{e_k \in R_i} K^{-1}(e_k)|}.$$

B3. Penalized Ratio of Covered Pairs: This measure is an extension of **B2**, where large reciprocal sets are penalized as in HYPERREC:

$$r(e_i, R_i) = \left(\frac{1}{|R_i|}\right)^\alpha \times \frac{|K(e_i) \cap \bigcup_{e_k \in R_i} K^{-1}(e_k)|}{|K(e_i) \cup \bigcup_{e_k \in R_i} K^{-1}(e_k)|}.$$

To demonstrate the necessity of the reciprocal-set penalty term $((1/|R_i|)^\alpha)$ and the normalizing term $|H_i|$ in Eq. (5), we consider two variants of HYPERREC where these two terms are removed respectively from Eq. (5).

B4. HyperRec w/o Normalization: This measure is a variant of HYPERREC where the normalization by $|H_i|$ is removed from Eq. (5) as follows:

$$r(e_i, R_i) = \left(\frac{1}{|R_i|}\right)^\alpha \left(|H_i| - \frac{\sum_{v_h \in H_i} \mathcal{L}(p_h, p_h^*)}{\mathcal{L}_{\max}} \right)$$

B5. HyperRec w/o Size Penalty: This measure is a variant of HYPERREC where the reciprocal-size penalty term $(1/|R_i|)^\alpha$ is removed from Eq. (5) as follows:

$$r(e_i, R_i) = 1 - \frac{\sum_{v_h \in H_i} \mathcal{L}(p_h, p_h^*)}{|H_i| \cdot \mathcal{L}_{\max}}$$

The baseline measures **B1 - B5** are other forms of arc-level reciprocity $r(e_i, R_i)$ given R_i . Below, we suggest two more baseline measures that are variants of HYPERREC with different ways of forming R_i .

B6. HyperRec w/ All Arcs as Reciprocal Set: This measure is a variant of HYPERREC where the reciprocal set is always defined as $R_i = E$.

B7. HyperRec w/ Inversely Overlapping Arcs as Reciprocal Set: This measure is a variant of HYPERREC where the reciprocal set is always defined as

$$R_i = \{e_k \in E : \min(|H_i \cap T_k|, |T_i \cap H_k|) \geq 1\}.$$

Table 2: HYPERREC satisfies all axioms, while all the others do not.
(a) Arc-level Axioms (B6 and B7 are exactly the same with HYPERREC regarding arc-level reciprocity)

Measure	Axioms				
	1	2	3	4	5
B1 (Pearcy et al. [2014])	✓	✓	✗	✓	✓
B2 (Ratio of Covered Pairs)	✓	✓	✗	✗	✓
B3 (Penalized Ratio of Covered Pairs)	✓	✓	✓	✗	✓
B4 (HYPERREC w/o Normalization)	✓	✓	✓	✓	✗
B5 (HYPERREC w/o Size Penalty)	✓	✓	✗	✓	✓
HYPERREC (proposed)	✓	✓	✓	✓	✓

(b) Hypergraph-level Axioms (B2-B5 are not applicable)

Measure	Axioms		
	6	7	8
B1 (Pearcy et al. [2014])	✗	✓	✓
B6 (HYPERREC w/ All Arcs as Reciprocal Set)	✗	✓	✗
B7 (HYPERREC w/ Inversely Overlapping Arcs as Reciprocal Set)	✓	✓	✗
HYPERREC (proposed)	✓	✓	✓

That is, **all** inversely overlapping arcs (see Section 3.1 for the definition) are used as the reciprocal set.

As summarized in Table 2, none of the considered baseline measures satisfies all the axioms, while HYPERREC satisfies all (Theorem 1). Refer to Appendix B for specific counter-examples for the baseline measures. Especially, the failure of **B6** and **B7** highlights the necessity of finding the maximum reciprocity value over all potential reciprocal arcs, as described in Eq (6), in order for HYPERREC to satisfy all the axioms.

3.4 Exact and Rapid Search for Reciprocal Sets

We propose FASTHYPERREC (**F**ast and **E**xact Algorithm for Hypergraph **R**eciprocity), an approach for rapidly searching for the reciprocal set R_i of Eq. (6). We prove the exactness of FASTHYPERREC and demonstrate its efficiency in real-world hypergraphs.

High-level ideas: The computational overhead of HYPERREC lies in finding the maximum reciprocity value over all possible subsets of the hyperarc set E (i.e., $\max_{R_i \subseteq E, R_i \neq \emptyset} r(e_i, R_i)$). Conducting an exhaustive search over the entire search space results in the time complexity of $O(2^{|E|})$, which becomes infeasible for the considered real-world hypergraphs (refer to Table 4 for the sizes of the real-world hypergraphs). To address this issue, FASTHYPERREC explores $2^{|\Psi_i|}$ instead of 2^E , where $\Psi_i \subseteq E$ holds, without affecting the computed reciprocity value. Specifically, FASTHYPERREC first creates disjoint groups of hyperarcs, which will be further explained in the following paragraph. Subsequently, it constructs Ψ_i by selecting solely the hyperarcs with the smallest head set size from each group. Then, FASTHYPERREC computes $\max_{R_i \subseteq \Psi_i, R_i \neq \emptyset} r(e_i, R_i)$. Importantly, $|\Psi_i| \ll |E|$ for most, if not all, real-world hypergraphs. That is, by employing FASTHYPERREC, the computation of $r(e_i, R_i)$ in HYPERREC is performed for a significantly smaller number of reciprocal sets R_i , leading to a substantial reduction in the overall computational time. Again, it is important to highlight that FASTHYPERREC is an exact algorithm that gives the precise value of Eq (7).

Detailed Procedure: FASTHYPERREC is described in Algorithm 1. For each arc e_i , we first retrieve the set Ω_i of inverse-overlapped arcs (see Section 3.1 for the definition) and check whether e_i is (1) non-reciprocal, (2) perfectly reciprocal, or (3) partially reciprocal. Reciprocity for the first two cases is 0 (lines 5-6) and 1 (lines 7-8), respectively. For a partially reciprocal case (lines 9-17), we group the arcs in

Algorithm 1: FASTHYPERREC for Exact and Rapid Computation of HYPERREC

Input: Hypergraph $G = (V, E)$
Output: The reciprocity $\{r(e_1), \dots, r(e_{|E|})\}$ of arcs in E

```

1 foreach  $e_i \in E$  do
2    $\Phi_i \leftarrow$  a mapping table whose default value is  $\emptyset$ 
3    $\Psi_i \leftarrow \{\}$ 
4    $\Omega_i \leftarrow \{e_j : \min(|H_i \cap T_j|, |T_i \cap H_i|) \geq 1\}$ 
5   if  $\Omega_i = \emptyset$  then
6      $r(e_i) \leftarrow 0$ 
7   else if  $\langle T_i, H_i \rangle \in \Omega_i$  then
8      $r(e_i) \leftarrow 1$ 
9   else
10    foreach  $e_k = \langle H_k, T_k \rangle \in \Omega_i$  do
11       $H'_i \leftarrow H_i \cap T_k;$ 
12       $T'_i \leftarrow T_i \cap H_k$ 
13       $\Phi_i(\langle H'_i, T'_i \rangle) \leftarrow \Phi_i(\langle H'_i, T'_i \rangle) \cup \{e_k\}$ 
14    foreach  $\langle H'_i, T'_i \rangle$  where  $\Phi_i(\langle H'_i, T'_i \rangle) \neq \emptyset$  do
15       $e'_i \leftarrow \operatorname{argmin}_{e_j \in \Phi_i(\langle H'_i, T'_i \rangle)} |H_j|$ 
16       $\Psi_i \leftarrow \Psi_i \cup \{e'_i\}$ 
17     $r(e_i) \leftarrow \max_{R_i \subseteq \Psi_i} r(e_i, R_i)$ 
18  return  $\{r(e_1), \dots, r(e_{|E|})\}$ 

```

 Table 3: Running time in seconds of FASTHYPERREC and searching Ω_i . O.O.T.: out of time (≥ 12 hours).

	metabolic		email		citation		qna		bitcoin		
	iAF1260b	iJO1366	enron	eu	data mining	software	math	server	2014	2015	2016
FASTHYPERREC	0.382	0.567	0.220	8.221	20.766	422.764	2.820	2.981	12297.318	762.645	428.283
Searching Ω_i	O.O.T.	O.O.T.	O.O.T.	O.O.T.	O.O.T.	O.O.T.	O.O.T.	O.O.T.	O.O.T.	O.O.T.	O.O.T.

Ω_i using a mapping table Φ_i where the key of each arc $e_k \in \Omega_i$ is the head-set and tail-set nodes of e_i that it covers (i.e., $\langle H'_i, T'_i \rangle$ where $H'_i \leftarrow H_i \cap T_k$ and $T'_i \leftarrow T_i \cap H_k$). For each group with the same key $\langle H'_i, T'_i \rangle$, we choose an arc with the minimum number of head set nodes. Then, we create a new search space Ψ_i containing only the chosen arcs. After that, every subset R_i of Ψ_i is considered to maximize Eq. (5), and we return the maximum value as the reciprocity $r(e_i)$ of e_i .

Theoretical Properties: As stated in Theorem 2, FASTHYPERREC finds the best reciprocal set, as in Eq. (6), and thus it computes the reciprocity of each arc exactly, as in Eq. (7).

Theorem 2 (Exactness of FASTHYPERREC). *For every $e_i \in E$, $\max_{R_i \subseteq E} r(e_i, R_i)$ is identical to the $\max_{R_i \subseteq \Psi_i} r(e_i, R_i)$.*

Proof. See Appendix A.3. □

For a special type of hypergraphs, we further reduce the search space based on Corollary 1. Recall that Ψ_i is a final search space produced by FASTHYPERREC.

Corollary 1. *Consider a hypergraph G where every arc's tail set size is 1 (i.e., $|T_i| = 1, \forall i \in \{1, \dots, |E|\}$), and let $\Gamma_{i,k}$ be a subset of Ψ_i that satisfies $|\Gamma_{i,k}| = k$ and $|H_s| \leq |H_t|, \forall e_s \in \Gamma_{i,k}, \forall e_t \in \{\Psi_i \setminus \Gamma_{i,k}\}$. Then, $\operatorname{argmax}_{(R_i \subseteq E \text{ s.t. } |R_i|=k)} r(e_i, R_i)$ is identical to $\Gamma_{i,k}, \forall k \in \{1, \dots, |\Psi_i|\}$, which implies that $\operatorname{argmax}_{R_i \subseteq \Psi_i, R_i \neq \emptyset} r(e_i, R_i)$ is identical to $\operatorname{argmax}_{R_i \in \{\Gamma_{i,1}, \dots, \Gamma_{i,|\Psi_i|}\}} r(e_i, R_i)$. That is, the size of the search space for R_i is reduced to $O(|\Psi_i|)$.*

Proof. See Appendix A.4. □

Complexity Analysis and Evaluation in Real-world Hypergraphs: After the reduction above, the size of the search space for R_i becomes $O(2^{|\Psi_i|})$ in general and $O(|\Psi_i|)$ for the case where every arc's tail set size is 1 (i.e., $|T_i| = 1, \forall i \in \{1, \dots, |E|\}$). Although the complexity is still exponential, we demonstrate that the search space is reasonably small, and thus a search can be performed within a

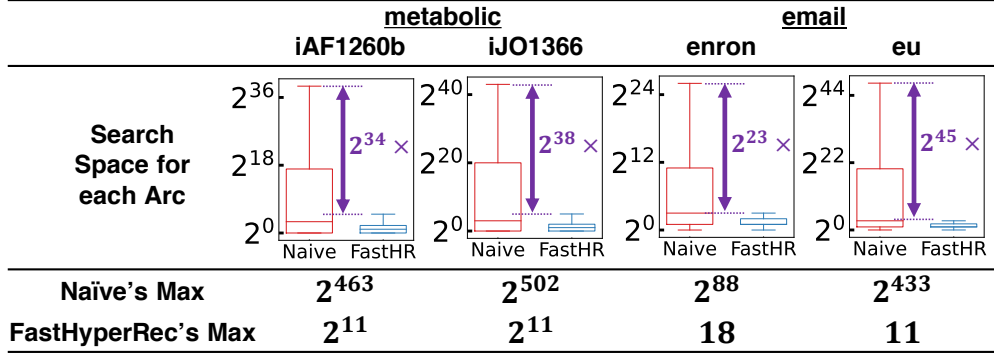


Figure 4: FASTHYPERREC (FastHR in short, left in each box plot) reduces the search space by up to $2^{491} (\approx 10^{147}) \times$, compared to that of the naive method (right in each box plot) in the iJO1366 dataset, which has 1,805 nodes and 2,251 arcs. To improve legibility, we remove several outliers that lie outside the interquartile range (refer to Footnote 3).

Table 4: Summary of 11 real-world hypergraphs from 5 domains: the number of nodes $|V|$, the number of arcs $|E|$, the average size of head set $|\overline{H_i}|$, the average size of tail set $|\overline{T_i}|$, the average node in-degree $|\overline{d_{in}(v)}|$ and the average node out-degree $|\overline{d_{out}(v)}|$.

Dataset	$ V $	$ E $	$ \overline{H_i} $	$ \overline{T_i} $	$ \overline{d_{in}(v)} $	$ \overline{d_{out}(v)} $
metabolic-iaf1260b	1,668	2,083	2.267	1.998	2.831	2.495
metabolic-iJO1366	1,805	2,251	2.272	2.026	2.833	2.527
email-enron	110	1,484	2.354	1.000	31.764	13.491
email-eu	986	35,772	2.368	1.000	85.900	36.280
citation-dm	27,164	73,113	3.038	3.253	8.177	8.755
citation-software	16,555	53,177	2.717	2.927	8.729	9.401
q&a-math	34,812	93,731	1.000	1.779	2.692	4.789
q&a-server	17,2330	27,2116	1.000	1.747	1.579	2.759
bitcoin-2014	1,697,625	1,437,082	1.697	1.478	1.437	1.251
bitcoin-2015	1,961,886	1,449,827	1.744	1.568	1.288	1.159
bitcoin-2016	2,009,978	1,451,135	1.715	1.495	1.238	1.079

reasonable time period for real-world hypergraphs. To evaluate the effectiveness of FASTHYPERREC, we compare the size of search space of FASTHYPERREC and a naive method that finds the best reciprocal set in Ω_i in four real-world hypergraphs, which are described in the following section. As shown in Figure 4,³ in the iJO1366 dataset, which has 1,805 nodes and 2,251 arcs, the naive method searches at most $2^{502} (\approx 10^{148})$ sets for the reciprocity of an arc, while FASTHYPERREC searches at most $2^{11} (= 2048)$ sets. In addition, we report the running time taken to compute the reciprocity of each of the 11 real-world hypergraphs, which are described in detail in the following section. As shown in Table 3, FASTHYPERREC terminates within 3.5 hours for every hypergraph, while naively searching Ω_i does not terminate within 12 hours for any of the hypergraphs.

Table 5: Hypergraph reciprocity $r(G)$ of 11 datasets when $\alpha \approx 0$, $\alpha = 0.5$, and $\alpha = 1$.

	metabolic		email		citation		q&a		bitcoin			
	iAF1260b	iJO1366	enron	eu	data mining	software	math	server	2014	2015	2016	
$r(G)$	$\alpha \approx 0$	21.455	22.533	59.161	79.489	12.078	15.316	9.608	13.219	10.829	6.923	3.045
	$\alpha = 0.5$	17.756	18.497	49.480	65.477	10.840	13.984	9.283	13.196	10.654	6.845	2.988
	$\alpha = 1.0$	16.654	17.385	44.459	58.139	10.585	13.704	9.236	13.193	10.606	6.828	2.977

Table 6: Hypergraph reciprocity $r(G)$ is robust to the choice of α . Although their absolute value may differ (see Table 5), their relative values are not sensitive to the choice of α , as supported by the fact that all the measured Pearson correlation coefficients and Spearman rank correlation coefficients are greater than 0.99.

		Pearson Correlation	Spearman Rank Correlation
$r(G)$	$\alpha \approx 0 \leftrightarrow \alpha = 0.5$	0.999	1.0
	$\alpha \approx 0 \leftrightarrow \alpha = 1.0$	0.999	0.991
	$\alpha = 0.5 \leftrightarrow \alpha = 1.0$	0.999	0.991

4 Datasets and Observations

In this section, we investigate the reciprocal patterns of real-world hypergraphs using HYPERREC and FASTHYPERREC. After introducing used real-world hypergraph datasets and null hypergraphs, we discuss our observations at three different levels: *hypergraph*, *arc*, and *node*. The significance of the patterns are verified by a comparison with the null hypergraphs.

4.1 Datasets and Null Hypergraphs

Datasets: We use 11 real-world hypergraphs from five different domains. Refer to Table 4 for basic statistics of them. All duplicated edges are removed, and detailed pre-processing steps are described in the Appendix C.

- **Metabolic** (iAF1260b and iJO1366 Yadati et al. [2020]): Each network models chemical reactions among various genes. Nodes correspond to genes, and arcs indicate reactions.
- **Emails** (email-enron Chodrow and Mellor [2020] and email-eu Leskovec and Krevl [2014]): Each node is an email account, and each arc consists of two ordered sets of senders and receivers of an email.
- **Citations** (DBLP-data mining and DBLP-software Sinha et al. [2015]). Each node is a researcher, and each head set and tail set indicates a paper. Arcs represent citations, as in Figure 1.
- **Question and Answering** (math-overflow and stack-exchange server fault Archive [2022]). Each node is a user, and each arc corresponds to a post. The questioner of a post becomes the head of an arc and the answerers compose its tail set.
- **Bitcoin Transactions** (bitcoin-2014, 2015, 2016 Wu et al. [2021]). Each node is an address in bitcoin transactions, and each arc is a transaction among users. The three datasets contain the first 1,500,000 transactions of Nov 2014, June 2015, and Jan 2016, respectively. We filtered out all transactions where the head set and the tail set are the same.

Null Hypergraphs: Patterns observed in real-world graphs can be caused by chance. In order to demonstrate discovered reciprocal characteristics are distinguishable from random behavior, we measure the same statistics and patterns in randomized hypergraphs, which we call *null hypergraphs*. Given a real hypergraph, we create a null hypergraph with the same number of nodes and the same distribution of arc sizes (i.e., the size of the head set and tail set of each arc). To create each arc, we draw nodes

³Note that, to improve legibility, we remove data points that lie outside the interquartile range (i.e., $[Q_1 - 1.5(Q_3 - Q_1), Q_3 + 1.5(Q_3 - Q_1)]$, where Q_3 and Q_1 denote the third and first quantile of the corresponding distribution) from the box plots.

Table 7: Observations 1 and the superiority of REDi. Reciprocity in (a) real-world hypergraphs, (b) null hypergraphs, (c) those generated by REDi (Section 5), and (d) those generated by a baseline generator is reported. Specifically, we generate five synthetic hypergraphs using each generator (Null, REDi, and Baseline) and the statistics from each dataset, and report the average ($\overline{r(G)}$) and standard deviation ($sd(r(G))$) of hypergraph-level reciprocity values of the generated hypergraphs. As the arc-level difference, we report the D-statistic (the lower the better) between each distribution of arc-level reciprocity and that in the corresponding real-world hypergraph. Values below 10^{-6} are all marked with *. In each column, the hypergraph reciprocity closest to that in the real-world hypergraph and the minimum D-statistic are underlined. Note that real-world hypergraphs are more reciprocal than null hypergraphs, and our proposed generator, REDi, successfully reproduces the reciprocity in real-world hypergraphs.

		metabolic		email		citation		q&a		bitcoin		
		iAF1260b	iJO1366	enron	eu	data mining	software	math	server	2014	2015	2016
Real World	$\overline{r(G)}$	21.455	22.533	59.001	79.416	12.078	15.316	9.608	13.219	10.829	6.923	3.045
Null	$\overline{r(G)}$	0.306	0.270	14.862	4.633	0.094	0.147	0.018	0.002	0.0001	0.000*	0.000*
	$sd(r(G))$	0.054	0.091	0.296	0.110	0.005	0.006	0.001	0.005	0.000*	0.000*	0.000*
	D-Stat	0.625	0.642	0.539	0.807	0.355	0.377	0.124	0.160	0.147	0.100	0.050
ReDi (Section 5)	$\overline{r(G)}$	<u>21.727</u>	<u>22.185</u>	<u>59.161</u>	<u>79.489</u>	<u>12.601</u>	<u>14.279</u>	<u>9.427</u>	<u>13.229</u>	<u>10.267</u>	<u>6.587</u>	<u>3.497</u>
	$sd(r(G))$	1.811	0.562	2.895	1.013	0.586	0.448	0.004	0.083	0.451	0.121	0.796
	D-Stat	<u>0.098</u>	<u>0.104</u>	<u>0.053</u>	<u>0.043</u>	<u>0.212</u>	<u>0.151</u>	<u>0.011</u>	<u>0.005</u>	<u>0.045</u>	<u>0.033</u>	<u>0.017</u>
Baseline (Section 5)	$\overline{r(G)}$	0.412	0.851	23.846	31.190	0.048	0.004	1.622	0.002	0.002	0.002	0.001
	$sd(r(G))$	0.117	0.882	1.437	0.273	0.642	0.543	0.004	0.009	0.002	0.002	0.002
	D-Stat	0.625	0.623	0.403	0.535	0.328	0.367	0.103	0.160	0.147	0.099	0.050

Table 8: P-value testing results on the 11 considered datasets. The null hypotheses are all rejected, which implies that real-world hypergraphs are significantly more reciprocal than null hypergraphs. A p-value smaller than 0.00001 is denoted by 0.0000*.

		metabolic		email		citation		q&a		bitcoin		
		iAF1260b	iJO1366	enron	eu	data mining	software	math	server	2014	2015	2016
Z-stat		-1502.52	-1789.79	-241.13	-3835.98	-17548.20	-9605.19	-8884.98	-88965.12	-691316.77	-555709.95	-325308.06
P-value		0.0000*	0.0000*	0.0000*	0.0000*	0.0000*	0.0000*	0.0000*	0.0000*	0.0000*	0.0000*	0.0000*
Null hypothesis		Reject	Reject	Reject	Reject	Reject	Reject	Reject	Reject	Reject	Reject	Reject

uniformly at random and compose a head set and a tail set with the chosen nodes. To minimize the randomness of experiments, we create 30 null hypergraphs from each dataset and report the statistics averaged over them.

4.2 Observations

We investigate the reciprocal patterns of real-world hypergraphs at three different levels: Hypergraph, Arc, and Node.

L1. Hypergraph Level: We first demonstrate that hypergraph reciprocity $r(G) = \frac{1}{|E|} \sum_{e_i \in E} r(e_i)$ is robust to the choice of α , i.e. the size penalty term for reciprocal sets. As shown in Table 6, although absolute reciprocity values vary depending on α , their ranks in real-world hypergraphs remain almost the same, as supported by the fact that both the Pearson and rank correlation coefficients are near 1. Based on this result, we fix α to a value near zero for the investigation below.

As shown in Table 7, the hypergraph reciprocity is several orders of magnitude greater in real-world hypergraphs than in corresponding null hypergraphs. To statistically verify this, we conduct statistical tests for all the datasets where the alternative hypothesis is that $\overline{r(G)}$ is statistically-significantly greater than $\overline{r(G_{null})}$. The detailed numerical results of the tests are provided in Table 8. In summary, we demonstrate that the hypergraph reciprocity is statistically-significantly greater in real-world hypergraphs than in corresponding null hypergraphs.

Observation 1. *Real-world hypergraphs are more reciprocal than randomized hypergraphs.*

L2. Arc Level: We first show the robustness of arc-level reciprocity to the choice of α , i.e. the size

Table 9: Arc-level reciprocity $r(e, R)$ is robust to the choice of α . Although their absolute values may differ, their relative values are not sensitive to the choice of α , as supported by the fact that the measured Pearson correlation coefficients and Spearman rank correlation coefficients are at least 0.678 and in many cases even close to 1.

		metabolic		email		citation		q&a		bitcoin		
		iAF1260b	iJO1366	enron	eu	data mining	software	math	server	2014	2015	2016
Pearson	$\alpha \approx 0 \leftrightarrow \alpha = 0.5$	0.961	0.957	0.928	0.836	0.984	0.986	0.994	0.999	0.997	0.998	0.997
	$\alpha \approx 0 \leftrightarrow \alpha = 1.0$	0.916	0.913	0.828	0.678	0.973	0.977	0.992	0.999	0.995	0.997	0.996
	$\alpha = 0.5 \leftrightarrow \alpha = 1.0$	0.985	0.986	0.975	0.967	0.998	0.998	0.999	0.999	0.999	0.999	0.999
Spearman Rank	$\alpha \approx 0 \leftrightarrow \alpha = 0.5$	0.973	0.969	0.947	0.817	0.998	0.998	0.999	0.999	0.999	0.999	0.999
	$\alpha \approx 0 \leftrightarrow \alpha = 1.0$	0.925	0.918	0.869	0.721	0.996	0.996	0.999	0.999	0.999	0.999	0.999
	$\alpha = 0.5 \leftrightarrow \alpha = 1.0$	0.975	0.973	0.978	0.983	0.999	0.999	0.999	0.999	0.999	0.999	0.999

penalty term for reciprocal sets. We measure the Pearson and Rank correlation coefficients between arc-level reciprocity values in each pair of settings with different α values (spec., $0.0 \leftrightarrow 0.5$, $0.0 \leftrightarrow 1.0$, and $0.5 \leftrightarrow 1.0$). As shown in Table 9, the correlation coefficients are at least 0.721 and in most cases close to 1, implying that relative values of arc-level reciprocity remain almost the same regardless of α values. Due to this robustness, **we fix α to a value close to 0 for all the following experiments.**

At the arc level, we examine the relations between the degree of arcs and their reciprocity. We define degrees at the arc level as follows:

$$\text{Head set out-degree: } d_{H,out}(e_i) = \frac{1}{|H_i|} \sum_{v \in H_i} d_{out}(v) \quad (8)$$

$$\text{Tail set in-degree: } d_{T,in}(e_i) = \frac{1}{|T_i|} \sum_{v \in T_i} d_{in}(v) \quad (9)$$

Refer to Section 2.1 for the definitions of $d_{out}(v)$ and $d_{in}(v)$. Then, we compare the distributional difference of these statistics (i.e., Eqs. (8) and (9)) between the arcs of zero reciprocity and those of non-zero reciprocity.

As shown in Figure 5, the degrees at arcs with non-zero reciprocity tend to be greater than those at arcs with zero reciprocity. This is intuitive since arcs where their head sets are frequently being pointed and tail sets are frequently pointing others tend to have higher chance to be reciprocal. Such tendency, however, is not clear in null hypergraphs.

Observation 2. *Arcs with non-zero reciprocity tend to have higher head set out-degree and tail set in-degree than arcs with zero reciprocity.*

L3. Node Level: Lastly, we investigate reciprocal patterns at the node level. A node is called *degree-balanced*, when its in-degree and out-degree are similar. One may suspect that degree-balanced nodes tend to be involved in highly reciprocal arcs, as the number of incoming arcs and outgoing arcs are similar at them. To verify this hypothesis, we measure the *degree balance of each node v* , which we define as $x(v) := \log(d_{in}(v) + 1) - \log(d_{out}(v) + 1)$, and measure *node-level reciprocity $r(v)$* , which we define as

$$r(v) = \frac{1}{|E_v|} \sum_{e_k \in E_v} r(e_k) \quad (10)$$

where $E_v = \{e_k : v \in (H_k \cup T_k)\}$ is the set of arcs where v is included in its head set or its tail set. Figure 6 shows how the average node-level reciprocity depends on the degree balance of nodes after applying the Savitzky–Golay filter [Savitzky and Golay, 1964] for smoothing the curves. The curves from the real-world hypergraphs are bell-shaped with maximum values around zero, implying node-level reciprocity gets larger as nodes’ in- and out-degrees become balanced. On the other hand, such a tendency is not clear in null hypergraphs.

Observation 3. *There is a tendency that degree-balanced nodes participate more in arcs with high reciprocity.*

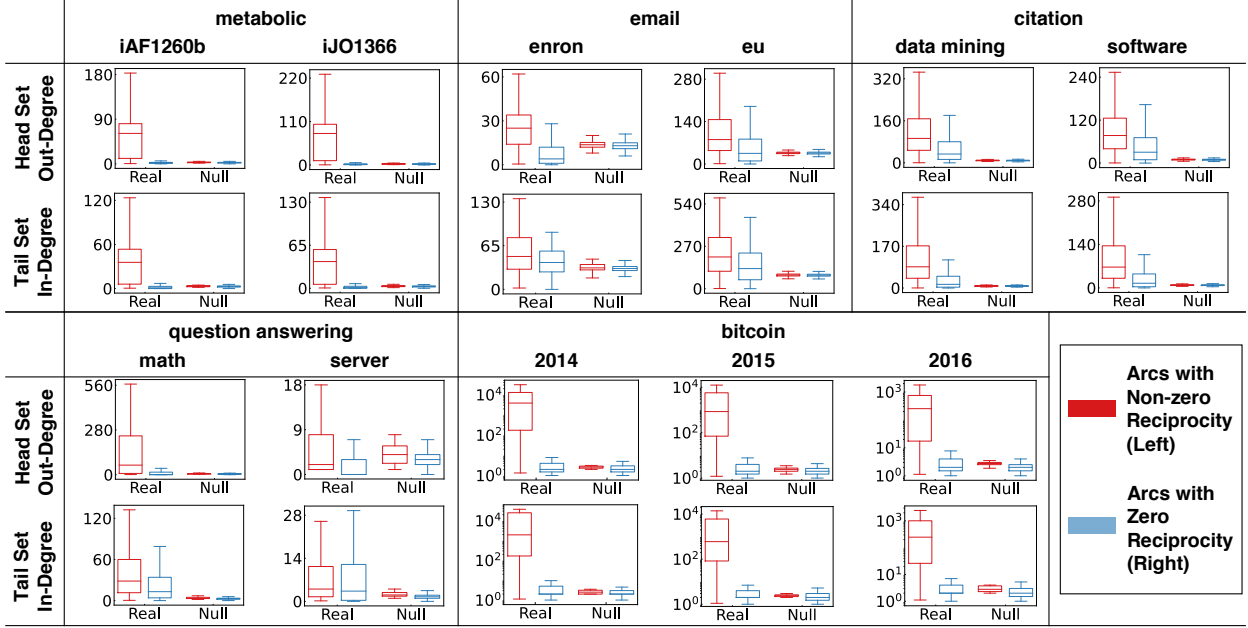


Figure 5: Observation 2. In real-world hypergraphs, the (a) head set out-degree and the (b) tail set in-degree tend to be larger at arcs with non-zero reciprocity (left in each box plot) than at arcs with zero reciprocity (right in each box plot), while there is no such trend in null hypergraphs.

5 Directed Hypergraph Generation: ReDi

In this section, we propose REDi (**R**eciprocal and **D**irectional Hypergraph Generator), a realistic generative model of directed hypergraphs. We first describe REDi. Then, we demonstrate its successful reproduction of the reciprocal properties of real-world hypergraphs examined in Section 4. In addition to testing our understanding of the patterns, REDi can also be used for anonymization, graph upscaling, etc [Leskovec, 2008].

5.1 Model Description

High-level Introduction to ReDi: Given some basic hypergraph statistics and three hyperparameter values, REDi generates a directed hypergraph with realistic structural and reciprocal patterns. REDi is largely based on HYPERPA [Do et al., 2020], an extension of the preferential attachment model [Albert and Barabási, 2002] to hypergraphs. In HYPERPA, each new node forms hyperedges with groups of nodes that are drawn with probability proportional to the degree of groups (i.e., the number of hyperedges containing each group). Introducing the degree of groups, instead of the degree of individual nodes, tends to lead to more realistic higher-order structures of generated graphs [Do et al., 2020]. REDi extends HYPERPA, which only can generate undirected hypergraphs, to generate directed hypergraphs and especially those with realistic reciprocal patterns. In a nutshell, REDi stochastically creates reciprocal arcs while controlling the number of reciprocal arcs and their degree of reciprocity.

Details of ReDi: The pseudocode of REDi is provided in Algorithm 2. It requires three hyperparameters: (a) a proportion $\beta_1 \in [0, 1]$ of reciprocal arc, (b) their extent $\beta_2 \in [0, 1]$ of reciprocity, and (c) the number N of initial nodes. In addition, REDi requires the following statistics that it preserves in expectation: (a) the number n of nodes, (b) the distributions f_{HD} and f_{TD} of the head-set and tail-set sizes, and (c) the distribution f_{NP} of the number of new arcs per node. We adopt NP distribution suggested in [Do et al., 2020] as our f_{NP} .

At each step, REDi introduces a new node v_i and creates k arcs where k is sampled from f_{NP} . Before creating a new arc, we decide whether it to be reciprocal (with prob. β_1) or ordinary. After deciding the size of a new arc according to the sizes sampled from f_{HD} and f_{TD} , we decide whether to include v into the head set (with prob. 0.5) or the tail set.

If a new arc is decided to be ordinary, we include v_i in either the head set or the tail set according

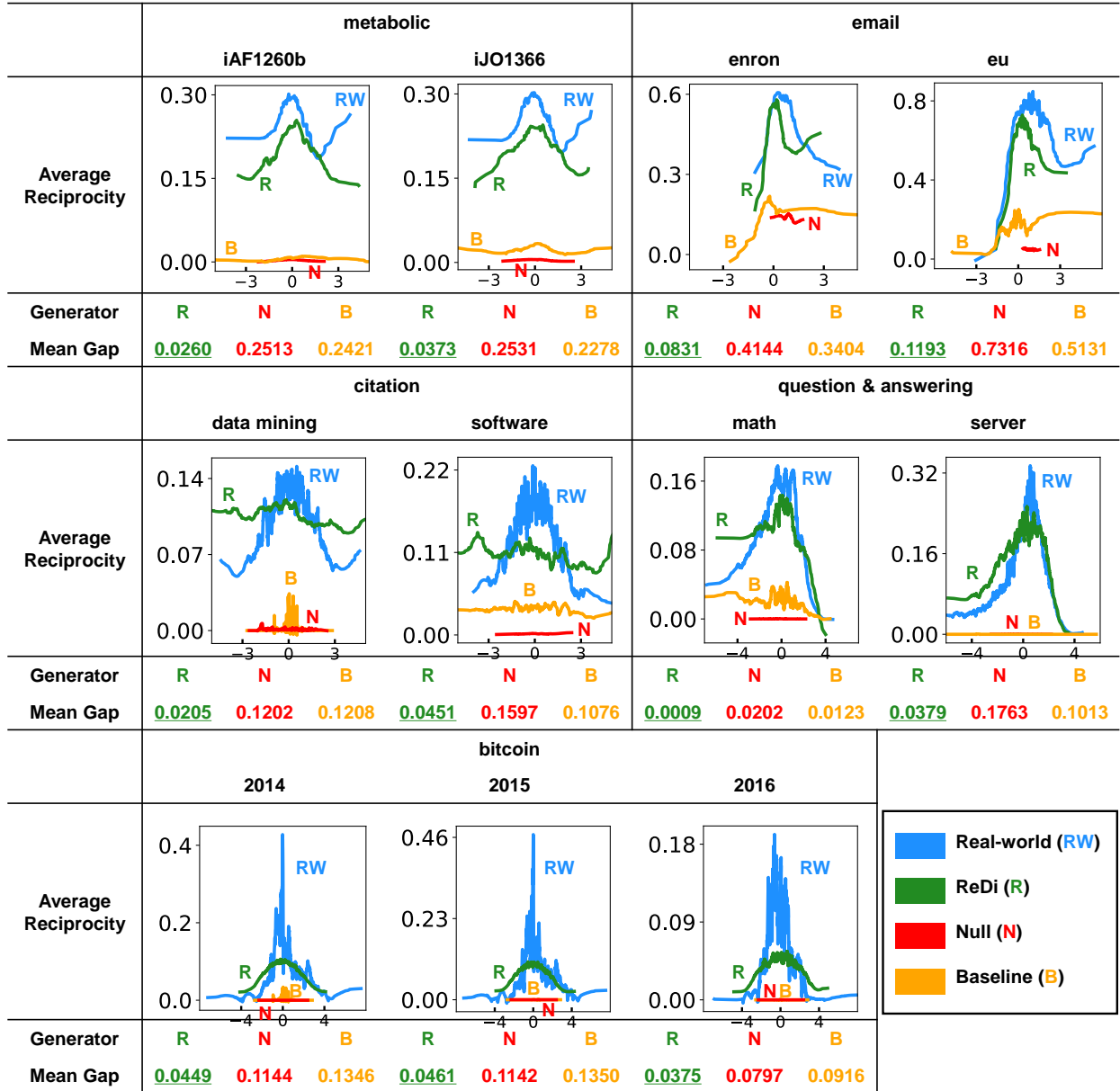


Figure 6: Observation 3 and the superiority of REDi. Relations between the degree balance and average reciprocity of nodes in real-world hypergraphs (RW), synthetic hypergraphs generated by REDi (R) (Section 5), null hypergraphs (N), and those generated by a baseline generator (B) are reported. For each dataset, we also report the mean gap values (Eq. (11)) from the real-world hypergraph. In real-world hypergraphs and those generated by REDi, node-level reciprocity tends to increase as nodes’ in- and out-degrees become balanced. The curves from the hypergraphs generated by REDi are most similar to those from real-world hypergraphs, as supported numerically by the smallest gaps from the real-world hypergraphs.

to the choice made beforehand. Subsequently, we fill the new arc with nodes sampled based on in- and out-degrees of groups (i.e., the number of arcs that include the group in their head set and tail set, respectively). Note that the head set and the tail set should be disjoint for both reciprocal and ordinary arcs.

If a new arc is decided to be reciprocal, we choose an opponent arc e_o uniformly at random among those with v_i (or among all existing arcs if no arc contains v_i). Then, we decide how many nodes are brought from the opponent arc’s head set and tail set by binomial sampling with probability $\beta_2 \in [0, 1]$.

Algorithm 2: REDI: Realistic Directed Hypergraph Generator

Input: (1) Number of nodes n and number of initial arcs N
(2) Distribution of hyperedge head, tail set size f_{HD}, f_{TD}
(3) Distribution of number of new hyperedges f_{NP}
(4) Reciprocal hyperparameter β_1 and β_2

Output: Generated hypergraph $G = (V, E)$.

- 1 Initialize G with N arcs (w/ 1 head & 1 tail) with $2N$ nodes
- 2 **foreach** node $v_i \in \{v_1, \dots, v_n\}$ **do**
- 3 $k \leftarrow$ a number sampled from f_{NP}
- 4 $V \leftarrow V \cup \{v_i\}$
- 5 $E_i \leftarrow \{\}$
- 6 **for** $j \leftarrow 1$ to k **do**
- 7 **while** *True* **do**
- 8 $recip. \leftarrow B(1, \beta_1)$; $head \leftarrow B(1, 0.5)^a$
- 9 $h, t \leftarrow$ arc sizes sampled from f_{HD}, f_{TD}
- 10 **if** $recip. = 0$ **then**
- 11 **if** $head = 1$ **then**
- 12 $H' \leftarrow \{v_i\}$; $T' \leftarrow \emptyset$
- 13 **else**
- 14 $T' \leftarrow \{v_i\}$; $H' \leftarrow \emptyset$
- 15 $H' \leftarrow H' \cup ((h - |H'|) \text{ nodes sampled}^b)$
- 16 $T' \leftarrow T' \cup ((t - |T'|) \text{ nodes sampled}^c)$
- 17 **else**
- 18 $e_o \leftarrow$ an arc sampled^d from E_i
- 19 $n_H \leftarrow B(\min(h, |T_o|), \beta_2)^a$
- 20 $H' \leftarrow \max(n_H, 1)$ nodes sampled^e from T_o
- 21 $n_T \leftarrow B(\min(t, |H_o|), \beta_2)^a$
- 22 $T' \leftarrow \max(n_T, 1)$ nodes sampled^f from H_o
- 23 **if** $head = 1$ and $h > |H'|$ **then**
- 24 $H' \leftarrow H' \cup \{v_i\}$
- 25 **else if** $head = 0$ and $t > |T'|$ **then**
- 26 $T' \leftarrow T' \cup \{v_i\}$
- 27 $H' \leftarrow H' \cup ((h - |H'|) \text{ nodes sampled}^b)$
- 28 $T' \leftarrow T' \cup ((t - |T'|) \text{ nodes sampled}^c)$
- 29 **if** $H' \cap T' = \emptyset$ **then**
- 30 **break** the while loop
- 31 $E \leftarrow E \cup \{H', T'\}$; $E_i = E_i \cup \{H', T'\}$
- 32 **return** $G = (V, E)$

^a $B(n, p)$ denotes binomial sampling with parameters n and p

^b with probability proportional to group in-degree [Do et al., 2020]

^c with probability proportional to group out-degree [Do et al., 2020]

^d uniformly at random from E_i (or from E if $E_i = \emptyset$)

^e with probability proportional to node in-degree

^f with probability proportional to node out-degree

After sampling nodes from the opponent arc with probability proportional to their degree, we fill the new arc with v_i and those sampled based on in- and out-degrees of groups.

5.2 Evaluation of ReDi

We evaluate how well REDI can reproduce the reciprocal patterns of real-world hypergraphs discussed in Section 4. For each real-world hypergraph, we generate 5 hypergraphs using their statistics and report

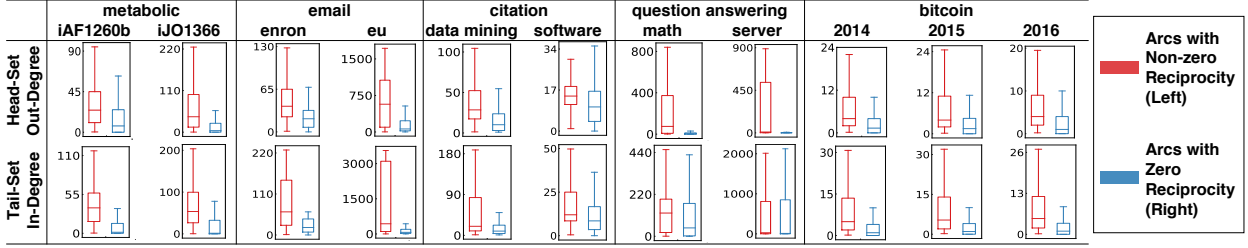


Figure 7: Hypergraphs generated by REDI exhibits Observation 2, which is a pervasive pattern in real-world hypergraphs, as shown in Figure 5

the average of generated statistics.⁴ In addition, we introduce a naive preferential attachment model, as a **baseline model** for comparison, to clarify the necessity of the reciprocal edge generation step. The baseline model is identical to REDI, except only for that it always decides to create ordinary arcs, i.e., $\beta_1 = \beta_2 = 0$.⁵

Reproducibility of Observation 1: We measure the reciprocity of generated hypergraphs at the hypergraph and arc levels and compare it with that of real-world hypergraphs. As shown in Table 7, REDI generates hypergraphs whose reciprocity is very close to that in the corresponding real-world hypergraphs both at the hypergraph and arc levels. The baseline model fails to reproduce high enough reciprocity in most cases.

Reproducibility of Observation 2: Moreover, as shown in Figure 7, in the hypergraphs generated by REDI, arcs with non-zero reciprocity tend to have higher (a) head set out-degree and (b) tail set in-degree than arcs with zero reciprocity, just as in the real-world hypergraphs.

Reproducibility of Observation 3: Furthermore, as shown in Figure 6, the bell-shaped relation between the degree balance and average reciprocity of nodes in hypergraphs generated by REDI is close to the relation in the corresponding real-world hypergraphs, as supported numerically by the smallest mean gaps (i.e., mean of squared differences) from the real-world hypergraphs. Formally, the mean gap is defined as follows:

$$\text{mean-gap}(f, f') = \frac{1}{|D|} \sum_{x \in D} (f(x) - f'(x))^2, \quad (11)$$

where D is the intersection of the domains of f and f' . Specifically, the mean gaps are up to $13\times$ smaller in hypergraphs generated by REDI than in those generated by the baseline model.

6 Conclusion

In this paper, we perform a systematic and extensive study of reciprocity in real-world hypergraphs. We propose HYPERREC, a family of probabilistic measures of reciprocity that guarantee all eight desirable properties (Table 2). Our algorithmic contribution is to develop FASTHYPERREC, which enables rapid yet exact computation of HYPERREC (Theorem 2, Figure 4, and Table 3). Using both, we discover several unique reciprocal patterns (Table 7 and Figures 5-6) that distinguish real-world hypergraphs from random hypergraphs. Lastly, we design REDI, a simple yet powerful generator that yields realistic directed hypergraphs (Table 7 and Figures 6-7). For **reproducibility**, we make the code and all datasets available at <https://github.com/kswoc97/hyprec>.

⁴The search space of β_1 is (a) $[0.05, 0.1, \dots, 0.6]$ for the small datasets where $|V| \leq 10^4$, and (b) $[0.001, 0.0015, \dots, 0.005]$ for the dense large datasets where $|V| > 10^4$ and $|E|/|V| \geq 3$, and (c) $[0.01, 0.02, \dots, 0.15]$ for the other sparse large datasets. The search space of β_2 is fixed to $\in [0.1, 0.1, \dots, 0.5]$ for all datasets.

⁵As bitcoin transactions are made among randomly chosen accounts, the repetition of (partial) group interactions is rarely observed. Due to this intrinsic characteristic of the datasets, we use the degrees of individual nodes instead of the degrees of groups when REDI and the baseline model are given the statistics from bitcoin datasets. The same strategy is also used for the baseline model when the input statistics are from the q&a server dataset. Without the strategy, the baseline model takes more than 12 hours.

Declarations

Competing interests

The authors have no relevant financial or non-financial interests to disclose.

References

- L. Akoglu, P. O. Vaz de Melo, and C. Faloutsos. Quantifying reciprocity in large weighted communication networks. In *Advances in Knowledge Discovery and Data Mining: 16th Pacific-Asia Conference, PAKDD 2012, Kuala Lumpur, Malaysia, May 29–June 1, 2012, Proceedings, Part II 16*, pages 85–96. Springer, 2012. doi: 10.1007/978-3-642-30220-6_8.
- R. Albert and A.-L. Barabási. Statistical mechanics of complex networks. *Reviews of modern physics*, 74(1):47, 2002. doi: 10.1103/RevModPhys.74.47.
- I. Archive. Stack Exchange Data Dump question answering dataset of stack exchange inc. <https://archive.org/details/stackexchange>, 2022.
- A. R. Benson, R. Abebe, M. T. Schaub, A. Jadbabaie, and J. Kleinberg. Simplicial closure and higher-order link prediction. *Proceedings of the National Academy of Sciences*, 115(48):E11221–E11230, 2018a. doi: 10.1073/pnas.1800683115.
- A. R. Benson, R. Kumar, and A. Tomkins. Sequences of sets. In *Proceedings of the 24th ACM SIGKDD International Conference on Knowledge Discovery & Data Mining*, pages 1148–1157, 2018b. doi: 10.1145/3219819.3220100.
- F. Bu, G. Lee, and K. Shin. Hypercore decomposition for non-fragile hyperedges: Concepts, algorithms, observations, and applications. *arXiv preprint arXiv:2301.08440*, 2023. doi: 10.48550/arXiv.2301.08440.
- P. Chodrow and A. Mellor. Annotated hypergraphs: models and applications. *Applied network science*, 5: 1–25, 2020. doi: 10.1007/s41109-020-0252-y.
- H. Choo and K. Shin. On the persistence of higher-order interactions in real-world hypergraphs. In *Proceedings of the 2022 SIAM International Conference on Data Mining (SDM)*, pages 163–171. SIAM, 2022. doi: 10.1137/1.9781611977172.19.
- D. Cirkovic, T. Wang, and S. Resnick. Preferential attachment with reciprocity: Properties and estimation. *arXiv preprint arXiv:2201.03769*, 2022. doi: 10.48550/arXiv.2201.03769.
- C. Comrie and J. Kleinberg. Hypergraph ego-networks and their temporal evolution. In *2021 IEEE International Conference on Data Mining (ICDM)*, pages 91–100. IEEE, 2021. doi: 10.1109/ICDM51629.2021.00019.
- M. T. Do, S.-e. Yoon, B. Hooi, and K. Shin. Structural patterns and generative models of real-world hypergraphs. In *Proceedings of the 26th ACM SIGKDD International Conference on Knowledge Discovery & Data Mining*, pages 176–186, 2020. doi: 10.1145/3394486.3403060.
- Y. Dong, W. Sawin, and Y. Bengio. Hnhn: Hypergraph networks with hyperedge neurons. *arXiv preprint arXiv:2006.12278*, 2020. doi: 10.48550/arXiv.2006.12278.
- D. Garlaschelli and M. I. Loffredo. Fitness-dependent topological properties of the world trade web. *Physical review letters*, 93(18):188701, 2004. doi: 10.1103/PhysRevLett.93.188701.
- C. A. Hidalgo and C. Rodríguez-Sickert. The dynamics of a mobile phone network. *Physica A: Statistical Mechanics and its Applications*, 387(12):3017–3024, 2008. doi: 10.1016/j.physa.2008.01.073.
- S. Kim, M. Choe, J. Yoo, and K. Shin. Reciprocity in directed hypergraphs: Measures, findings, and generators. In *The 22nd IEEE International Conference on Data Mining, ICDM 2022*. IEEE Computer Society, 2022. doi: 10.1109/ICDM54844.2022.00122.
- Y. Kook, J. Ko, and K. Shin. Evolution of real-world hypergraphs: Patterns and models without oracles. In *2020 IEEE International Conference on Data Mining (ICDM)*, pages 272–281. IEEE, 2020. doi: 10.1109/ICDM50108.2020.00036.

- G. Lee and K. Shin. Thyme+: Temporal hypergraph motifs and fast algorithms for exact counting. In *2021 IEEE International Conference on Data Mining (ICDM)*, pages 310–319. IEEE, 2021. doi: 10.1109/ICDM51629.2021.00042.
- G. Lee, J. Ko, and K. Shin. Hypergraph motifs: Concepts, algorithms, and discoveries. *PVLDB*, 13(12): 2256–2269, 2020. doi: 10.14778/3407790.3407823.
- G. Lee, M. Choe, and K. Shin. How do hyperedges overlap in real-world hypergraphs?-patterns, measures, and generators. In *Proceedings of the Web Conference 2021*, pages 3396–3407, 2021. doi: 10.1145/3442381.3450010.
- J. Leskovec. *Dynamics of large networks*. Carnegie Mellon University, 2008.
- J. Leskovec and A. Krevl. SNAP Datasets: Stanford large network dataset collection. <http://snap.stanford.edu/data>, June 2014.
- J. Lin. Divergence measures based on the shannon entropy. *IEEE Transactions on Information theory*, 37(1):145–151, 1991. doi: 10.1109/18.61115.
- X. Luo, J. Peng, and J. Liang. Directed hypergraph attention network for traffic forecasting. *IET Intelligent Transport Systems*, 16(1):85–98, 2022. doi: 10.1049/itr2.12130.
- M. E. Newman, S. Forrest, and J. Balthrop. Email networks and the spread of computer viruses. *Physical Review E*, 66(3):035101, 2002. doi: 10.1103/PhysRevE.66.035101.
- V.-A. Nguyen, E.-P. Lim, H.-H. Tan, J. Jiang, and A. Sun. Do you trust to get trust? a study of trust reciprocity behaviors and reciprocal trust prediction. In *Proceedings of the 2010 SIAM international conference on data mining*, pages 72–83. SIAM, 2010. doi: 10.1137/1.9781611972801.7.
- N. Percy, J. J. Crofts, and N. Chuzhanova. Hypergraph models of metabolism. *International Journal of Biological, Veterinary, Agricultural and Food Engineering*, 8(8):752–756, 2014. doi: 10.5281/zenodo.1094247.
- S. Ranshous, C. A. Joslyn, S. Kreyling, K. Nowak, N. F. Samatova, C. L. West, and S. Winters. Exchange pattern mining in the bitcoin transaction directed hypergraph. In *Financial Cryptography and Data Security: FC 2017 International Workshops, WAHC, BITCOIN, VOTING, WTSC, and TA, Sliema, Malta, April 7, 2017, Revised Selected Papers 21*, pages 248–263. Springer, 2017. doi: 10.1007/978-3-319-70278-0.16.
- A. Savitzky and M. J. Golay. Smoothing and differentiation of data by simplified least squares procedures. *Analytical chemistry*, 36(8):1627–1639, 1964. doi: 10.1021/ac60214a047.
- A. Sinha, Z. Shen, Y. Song, H. Ma, D. Eide, B.-J. Hsu, and K. Wang. An overview of microsoft academic service (mas) and applications. In *Proceedings of the 24th international conference on world wide web*, pages 243–246, 2015. doi: 10.1145/2740908.2742839.
- T. Squartini, F. Picciolo, F. Ruzzenenti, and D. Garlaschelli. Reciprocity of weighted networks. *Scientific reports*, 3(1):1–9, 2013. doi: 10.1038/srep02729.
- T. Wang and S. I. Resnick. Asymptotic dependence of in-and out-degrees in a preferential attachment model with reciprocity. *Extremes*, pages 1–34, 2022. doi: 10.1007/s10687-022-00439-5.
- Wikipedia. Computer Science Conference wikipedia. https://en.wikipedia.org/wiki/List_of_computer_science_conferences, 2022.
- J. Wu, J. Liu, W. Chen, H. Huang, Z. Zheng, and Y. Zhang. Detecting mixing services via mining bitcoin transaction network with hybrid motifs. *IEEE Transactions on Systems, Man, and Cybernetics: Systems*, 52(4):2237–2249, 2021. doi: 10.1109/TSMC.2021.3049278.
- N. Yadati, V. Nitin, M. Nimishakavi, P. Yadav, A. Louis, and P. Talukdar. Nhp: Neural hypergraph link prediction. In *Proceedings of the 29th ACM International Conference on Information & Knowledge Management*, pages 1705–1714, 2020. doi: 10.1145/3340531.3411870.

N. Yadati, T. Gao, S. Asoodeh, P. Talukdar, and A. Louis. Graph neural networks for soft semi-supervised learning on hypergraphs. In *Advances in Knowledge Discovery and Data Mining: 25th Pacific-Asia Conference, PAKDD 2021, Virtual Event, May 11–14, 2021, Proceedings, Part I*, pages 447–458. Springer, 2021. doi: 10.1007/978-3-030-75762-5_36.

S.-e. Yoon, H. Song, K. Shin, and Y. Yi. How much and when do we need higher-order information in hypergraphs? a case study on hyperedge prediction. In *Proceedings of The Web Conference 2020*, pages 2627–2633, 2020. doi: 10.1145/3366423.3380016.

A Appendix: Proof of Theorems

In this section, we provide proofs of theorems in the main paper. We first introduce some preliminaries of proofs and then prove why HYPERREC, the proposed family of reciprocity measures, satisfies all of **Axioms 1-8**. Then, we prove the exactness of **FastHyperRec** and the related complexity reduction techniques.

A.1 Preliminaries of Proofs

In this subsection, we first give the general form of our proposed measure. Then, we introduce several important characteristics of *Jensen-Shannon Divergence* (JSD) [Lin, 1991], which plays a key role in our proofs. After that, we examine how these concepts are applied to our measure. Basic symbols used for hypergraphs and arcs are defined in Section 2.1.

HYPERREC, the proposed reciprocity measure for an arc e_i and for a hypergraph G is defined as

$$r(e_i) := \max_{R_i \subseteq E, R_i \neq \emptyset} \left(\frac{1}{|R_i|} \right)^\alpha \left(1 - \frac{\sum_{v_h \in H_i} \mathcal{L}(p_h, p_h^*)}{|H_i| \cdot \mathcal{L}_{max}} \right), \quad (12)$$

$$r(G) := \frac{1}{|E|} \sum_{i=1}^{|E|} r(e_i), \quad (13)$$

where $\mathcal{L}(p_h, p_h^*)$ denotes Jensen-Shannon Divergence [Lin, 1991] between a transition probability distribution p_h and the optimal transition probability distribution p_h^* .

For a target arc e_j with an arbitrary non-empty reciprocal set R_j , the transition probability is defined as

$$p_h(v) = \begin{cases} \frac{\sum_{e_k \in R_j} \left(\frac{\mathbf{1}[v_h \in T_k, v \in H_k]}{|H_k|} \right)}{\sum_{e_k \in R_j} (\mathbf{1}[v_h \in T_k])} & \text{if } v_h \in \bigcup_{e_k \in R_j} T_k, \\ 1 & \text{if } v = v_{sink} \text{ and } v_h \notin \bigcup_{e_k \in R_j} T_k, \\ 0 & \text{otherwise,} \end{cases}$$

where $\mathbf{1}[\text{TRUE}] = 1$, and $\mathbf{1}[\text{FALSE}] = 0$.

In Lemma 1, we provide several theoretical properties of JSD that are used for our proofs. Note that a general form of $\text{JSD}(P \parallel Q)$ is defined as

$$\mathcal{L}(P, Q) = \sum_{i=1}^n \ell(p_i, q_i), \quad (14)$$

where

$$\ell(p_i, q_i) = \frac{p_i}{2} \log \frac{2p_i}{p_i + q_i} + \frac{q_i}{2} \log \frac{2q_i}{p_i + q_i}. \quad (15)$$

Lemma 1 (Basic Properties of Jensen-Shannon Divergence). *The Jensen-Shannon Divergence (JSD) has the following properties:*

- **A-I.** For any two discrete probability distributions P and Q , $0 \leq \text{JSD}(P \parallel Q) \leq \log 2$ holds.
- **A-II.** For two discrete probability distributions P and Q where their non-zero-probability domains do not overlap (i.e., $p_i q_i = 0, \forall i = \{1, \dots, |V|\}$), $\text{JSD}(P \parallel Q)$ is maximized, and the maximum value is $\log 2$.
- **A-III.** Consider two discrete probability distributions P and Q . If there exists a value where both P and Q have non-zero probability, $\text{JSD}(P \parallel Q) < \log 2$ holds.

Proof. • **(Proof of A-I)** Refer to [Lin, 1991] for a proof of **A-I**.

- **(Proof of A-II)** Let \mathcal{X}_p be the domain where P has non-zero probability, and let \mathcal{X}_q be the domain where Q has non-zero probability. Since \mathcal{X}_p and \mathcal{X}_q do not overlap, Eq. (14) is rewritten as

$$\mathcal{L}(P, Q) = \sum_{i \in \mathcal{X}_p} \frac{p_i}{2} \log 2 + \sum_{i \in \mathcal{X}_q} \frac{q_i}{2} \log 2 = \frac{\log 2}{2} \left(\sum_{i \in \mathcal{X}_p} p_i + \sum_{i \in \mathcal{X}_q} q_i \right) = \log 2.$$

- **(Proof of A-III)** Let k be a point where $p_k q_k \neq 0$ holds. Then, Eq. (14) is rewritten as

$$\mathcal{L}(P, Q) \leq \sum_{i \in \mathcal{X}_p \setminus k} \frac{p_i}{2} \log 2 + \sum_{i \in \mathcal{X}_q \setminus k} \frac{q_i}{2} \log 2 + \left(\frac{p_k}{2} \log \frac{2p_k}{p_k + q_k} + \frac{q_k}{2} \log \frac{2q_k}{p_k + q_k} \right). \quad (16)$$

The below inequality implies that Eq. (16) is smaller than $\log 2$.

$$\begin{aligned} & \left(\frac{p_k}{2} \log 2 + \frac{q_k}{2} \log 2 \right) - \left(\frac{p_k}{2} \log \frac{2p_k}{p_k + q_k} + \frac{q_k}{2} \log \frac{2q_k}{p_k + q_k} \right) > 0 \\ & \equiv \frac{p_k}{2} \log \left(1 + \frac{q_k}{p_k} \right) + \frac{q_k}{2} \log \left(1 + \frac{p_k}{q_k} \right) > 0 \quad (\because p_k, q_k > 0). \end{aligned}$$

Since $\log(x) > 0$ holds for any $x > 1$, the last inequality holds. Thus, we can conclude that $\text{JSD}(P \parallel Q) < \log 2$ holds in this case. \square

In Lemma 2, we provide several basic properties of HYPERREC, our proposed measure of reciprocity in hypergraphs.

Lemma 2 (Basic Properties of HYPERREC). HYPERREC (i.e., defining $r(e_i, R_i)$ as in Eq. (5)) has the following properties:

- **A-IV.** If a target arc's head set and the tail sets of its reciprocal arcs do not overlap, the target arc's reciprocity becomes zero. Formally,

$$\text{If } H_i \cap \bigcup_{e_k \in R_i} T_k = \emptyset \quad \text{then} \quad r(e_i, R_i) = 0.$$

- **A-V.** If a target arc's tail set and the head sets of its reciprocal arcs do not overlap, the target arc's reciprocity becomes zero. Formally,

$$\text{If } T_i \cap \bigcup_{e_k \in R_i} H_k = \emptyset \quad \text{then} \quad r(e_i, R_i) = 0.$$

- **A-VI.** If (a) a target arc's head set and the tail sets of its reciprocal arcs overlap and (b) the target arc's tail set and the head sets of its reciprocal arcs overlap, then the target arc's reciprocity is greater than zero. Formally,

$$\text{If } \sum_{e_k \in R_i} |H_i \cap T_k| \cdot |T_i \cap H_k| \geq 1 \quad \text{then} \quad r(e_i, R_i) > 0.$$

Proof. Below, we use \mathcal{L}_{max} to denote the maximum value of JSD, which is $\log 2$.

- **(Proof of A-IV)** For this case, as mentioned in Section 3.2, the probability mass is non-zero only at v_{sink} . On the other hand, the optimal transition probability p^* is non-zero only at each $v \in T_i$. Since $v_{sink} \notin T_i$, the non-zero-probability domains of the transition probability and the optimal transition probability do not overlap, and by **A-II**, the probabilistic distance between them is maximized. This happens for all $v \in H_i$. Therefore,

$$\begin{aligned} r(e_i, R_i) &= \left(\frac{1}{|R_i|} \right)^\alpha \left(1 - \frac{\sum_{v_h \in H_i} \mathcal{L}_{max}}{|H_i| \cdot \mathcal{L}_{max}} \right) \\ &= \left(\frac{1}{|R_i|} \right)^\alpha \left(1 - \frac{|H_i| \cdot \mathcal{L}_{max}}{|H_i| \cdot \mathcal{L}_{max}} \right) = \left(\frac{1}{|R_i|} \right)^\alpha \times 0 = 0. \end{aligned}$$

- **(Proof of A-V)** As in **A-IV**, the non-zero probability domains of the transition probability and the optimal transition probability do not overlap since $T_i \cap \bigcup_{e_k \in R_i} H_k = \emptyset$. Again, the probabilistic distance is maximized. This happens for all H_i , i.e.,

$$\begin{aligned} r(e_i, R_i) &= \left(\frac{1}{|R_i|} \right)^\alpha \left(1 - \frac{\sum_{v_h \in H_i} \mathcal{L}^{max}}{|H_i| \cdot \mathcal{L}^{max}} \right) \\ &= \left(\frac{1}{|R_i|} \right)^\alpha \left(1 - \frac{|H_i| \cdot \mathcal{L}^{max}}{|H_i| \cdot \mathcal{L}^{max}} \right) = 0 \end{aligned}$$

- **(Proof of A-VI)** According to the statement, there exists at least one reciprocal arc e_k whose (a) tail set overlaps with the target arc's head set (i.e., $|T_k \cap H_i| \geq 1$) and (b) head set overlaps with the target arc's tail set (i.e., $|H_k \cap T_i| \geq 1$). Thus, for $v_h \in H_i \cap T_k$, p_h and p_h^* share non-zero probability domains, which implies $\mathcal{L}(p_h, p_h^*) < \log 2$ by **A-III**. Hence, we can derive the following inequality:

$$\begin{aligned} r(e_i, R_i) &= \left(\frac{1}{|R_i|} \right)^\alpha \left(1 - \frac{\sum_{v_h \in H_i} \mathcal{L}(p_h, p_h^*)}{|H_i| \cdot \mathcal{L}^{max}} \right) \\ &> \left(\frac{1}{|R_i|} \right)^\alpha \left(1 - \frac{|H_i| \cdot \mathcal{L}^{max}}{|H_i| \cdot \mathcal{L}^{max}} \right) = 0. \end{aligned}$$

□

A.2 Proof of Theorem 1.

In this section, we show that the proposed measure HYPERREC satisfies all the generalized axioms. For a proof of **Generalized Axiom 1**, we simply show that the former's reciprocity gets zero (i.e., $r(e_i, R_i) = 0$), while the latter's reciprocity gets a positive value (i.e., $r(e_j, R_j) > 0$). For proofs of **Generalized Axioms 2-4**, we first show how the formal statement of each axiom can be written in terms of the probabilistic distance. Then, we derive a less reciprocal case has a higher probabilistic distance between the transition probability and the optimal transition probability for every head set node of a target arc.

A.2.1 Proof of the Fact that HyperRec Satisfies Axiom 1

Through an example, **Axiom 1** states that an arc that has at least one inversely-overlapping arc should be more reciprocal than an arc without any inversely-overlapping arc. The generalized statement of **Axiom 1** is formalized in **Generalized Axiom 1**.

Proposition 1. HYPERREC (i.e., defining $r(e_i, R_i)$ as in Eq. (5)) satisfies Generalized Axiom 1.

Proof. We first show that $r(e_i, R_i) = 0$. The suggested condition ($\forall e'_i \in R_i : \min(|H_i \cap T'_i|, |T_i \cap H'_i|) = 0$) implies that every reciprocal arc $e'_i \in R_i$ lies in one of the following cases (for simplicity, we refer to $e'_i \in R_i$ as a *non-influential* arc if e'_i does not contribute to making the non-zero probability domains of the transition probability that overlap with that of the optimal transition probability): (1) When $(H_i \cap T'_i = \emptyset) \wedge (T_i \cap H'_i \neq \emptyset)$ holds, as shown in the proof of **A-IV**, e'_i is *non-influential*. (2) When $(H_i \cap T'_i \neq \emptyset) \wedge (T_i \cap H'_i = \emptyset)$ holds, as shown in the proof of **A-V**, e'_i is *non-influential*. (3) When $(H_i \cap T'_i = \emptyset) \wedge (T_i \cap H'_i = \emptyset)$ holds, as shown in the proof of **A-II** and **A-V**, e'_i is *non-influential*. That is, all reciprocal hyperarcs in R_i are *non-influential*, and by **A-II**, the distance between the transition probability and the optimal transition probability is maximized. This happens for all $v \in H_i$. Therefore,

$$\begin{aligned} r(e_i, R_i) &= \left(\frac{1}{|R_i|} \right)^\alpha \left(1 - \frac{\sum_{v_h \in H_i} \mathcal{L}^{max}}{|H_i| \cdot \mathcal{L}^{max}} \right) \\ &= \left(\frac{1}{|R_i|} \right)^\alpha \left(1 - \frac{|H_i| \cdot \mathcal{L}^{max}}{|H_i| \cdot \mathcal{L}^{max}} \right) = \left(\frac{1}{|R_i|} \right)^\alpha \times 0 = 0. \end{aligned}$$

We now show that $r(e_j, R_j) > 0$ holds. The suggested condition ($\exists e'_i \in R_i : \min(|H_i \cap T'_i|, |T_i \cap H'_i|) \geq 1$) is equivalent to the condition of **A-VI**. Thus, by **A-VI**, the inequality $r(e_j, R_j) > 0$ holds. Since $r(e_i, R_i) = 0$ and $r(e_j, R_j) > 0$, the following inequality holds: $r(e_i, R_i) < r(e_j, R_j)$. □

A.2.2 Proof of the Fact that HyperRec Satisfies Axiom 2

Through an example, **Axiom 2** states that an arc that inversely overlaps with reciprocal arcs to a greater extent should be more reciprocal. In addition, **Axiom 2** is divided into two cases, which are formalized in **Generalized Axiom 2A** and **2B** respectively.

Proposition 2A. HYPERREC (i.e., defining $r(e_i, R_i)$ as in Eq. (5)) satisfies Generalized Axiom 2A.

Proof. Since $|R_i| = |R_j| = 1$, the cardinality penalty terms on both sides can be discarded, i.e.,

$$r(e_i, R_j) = \left(\frac{1}{|R_i|} \right)^\alpha \left(1 - \frac{\sum_{v_i \in H_i} \mathcal{L}(p_h, p_h^*)}{|H_i| \cdot \mathcal{L}_{max}} \right) = 1 - \frac{\sum_{v_i \in H_i} \mathcal{L}(p_h, p_h^*)}{|H_i| \cdot \mathcal{L}_{max}}.$$

Since $|H_i| = |H_j|$, the main inequality is rewritten as

$$\begin{aligned} r(e_i, R_i) &< r(e_j, R_j) \\ &\equiv \sum_{v_h \in H_i} \mathcal{L}(p_h, p_h^*) > \sum_{v_h \in H_j} \mathcal{L}(p_h, p_h^*). \end{aligned} \quad (17)$$

Each head set can be divided into two parts: $H_k \setminus T'_k$ and $H_k \cap T'_k$, $\forall k = i, j$. For $H_k \setminus T'_k$, as described in **A-IV**, the probabilistic distance is maximized to $\mathcal{L}_{max} = \log 2$. For $H_k \cap T'_k$, by using the fact that $T_k \cap H'_k \neq \emptyset$, $\forall k = i, j$, we can derive $\mathcal{L}(p_h, p_h^*) < \log 2$ holds, $\forall v_h \in H_k \cap T'_k$, $\forall k = i, j$ by **A-VI**. One more notable fact is that, since there is a single reciprocal arc for the target arc, $\mathcal{L}(p_h, p_h^*)$ is the same for every $v_h \in H_k \cap T'_k$. Here, let $\bar{p}_k, \forall k = i, j$ be the transition probability distribution regarding the target arc e_k and its reciprocal set R_k . We rewrite the inequality (17)

$$\begin{aligned} \sum_{v_h \in H_i} \mathcal{L}(p_h, p_h^*) &> \sum_{v_h \in H_j} \mathcal{L}(p_h, p_h^*) \\ &\equiv |H_i \setminus T'_i| \times \log 2 + |H_i \cap T'_i| \times \mathcal{L}(\bar{p}_i, \bar{p}_i^*) > |H_j \setminus T'_j| \times \log 2 + |H_j \cap T'_j| \times \mathcal{L}(\bar{p}_j, \bar{p}_j^*). \end{aligned}$$

Below, we show that this inequality holds for Case (i) and then Case (ii).

Case (i): For Case (i), we first show that the inequality (17) is equivalent to $\mathcal{L}(\bar{p}_i, \bar{p}_i^*) > \mathcal{L}(\bar{p}_j, \bar{p}_j^*)$. The intersection of the target arc's head set and the reciprocal arc's tail set is larger for e_j than for e_i . Thus, the following inequality hold:

$$|H_i \setminus T'_i| \times \log 2 + |H_i \cap T'_i| \times \mathcal{L}(\bar{p}_i, \bar{p}_i^*) \geq |H_j \setminus T'_j| \times \log 2 + |H_j \cap T'_j| \times \mathcal{L}(\bar{p}_i, \bar{p}_i^*).$$

Therefore, Eq. (17) is implied by

$$\begin{aligned} |H_j \setminus T'_j| \times \log 2 + |H_j \cap T'_j| \times \mathcal{L}(\bar{p}_i, \bar{p}_i^*) &> |H_j \setminus T'_j| \times \log 2 + |H_j \cap T'_j| \times \mathcal{L}(\bar{p}_j, \bar{p}_j^*) \\ &\equiv |H_j \cap T'_j| \times \mathcal{L}(\bar{p}_i, \bar{p}_i^*) > |H_j \cap T'_j| \times \mathcal{L}(\bar{p}_j, \bar{p}_j^*) \\ &\equiv \mathcal{L}(\bar{p}_i, \bar{p}_i^*) > \mathcal{L}(\bar{p}_j, \bar{p}_j^*). \end{aligned}$$

Now, we show that $\mathcal{L}(\bar{p}_i, \bar{p}_i^*) > \mathcal{L}(\bar{p}_j, \bar{p}_j^*)$ holds. To this end, denote the size of the intersection regions as $F_1 = |T_i \cap H'_i| < F_2 = |T_j \cap H'_j|$. We can decompose the domain of $v \in V$ into four parts as

$$T_k \cap H'_k, \quad T_k \setminus H'_k, \quad H'_k \setminus T_k, \quad \text{and } V \setminus \{H'_k \cup T_k\}, \quad \forall k = i, j$$

For the last part, both the transition probability and the optimal transition probability of it have zero mass, i.e., $p_h(v) = p_h^*(v) = 0$, which results in no penalty. We only need to consider the first three parts for comparison. Here, the probabilistic distance can be explicitly written as

$$\begin{aligned} \mathcal{L}(\bar{p}_i, \bar{p}_i^*) &= F_1 \times \ell \left(\frac{1}{T}, \frac{1}{A} \right) + (A - F_1) \times \frac{1}{2A} \log 2 + (T - F_1) \times \frac{1}{2T} \log 2, \\ \mathcal{L}(\bar{p}_j, \bar{p}_j^*) &= F_2 \times \ell \left(\frac{1}{T}, \frac{1}{A} \right) + (A - F_2) \times \frac{1}{2A} \log 2 + (T - F_2) \times \frac{1}{2T} \log 2, \end{aligned}$$

where ℓ denotes a single-element comparison of $\text{JSD}(P \parallel Q)$ in Eq. (15). Let $A = |H'_i| = |H'_j|$ and $T = |T_i| = |T_j|$. Then, we can rewrite $\mathcal{L}(\bar{p}_i, \bar{p}_i^*) - \mathcal{L}(\bar{p}_j, \bar{p}_j^*) > 0$ as

$$\begin{aligned}
& \mathcal{L}(\bar{p}_i, \bar{p}_i^*) - \mathcal{L}(\bar{p}_j, \bar{p}_j^*) > 0 \\
& \equiv (F_1 - F_2) \times \ell \left(\frac{1}{T}, \frac{1}{A} \right) + (F_2 - F_1) \times \left(\frac{1}{2A} + \frac{1}{2T} \right) \log 2 > 0 \\
& \equiv (F_2 - F_1) \times \left(\frac{1}{2A} \log 2 + \frac{1}{2T} \log 2 - \ell \left(\frac{1}{T}, \frac{1}{A} \right) \right) > 0 \\
& \equiv \left(\frac{1}{2A} \log 2 - \frac{1}{2A} \log \frac{2T}{A+T} + \frac{1}{2T} \log 2 - \frac{1}{2T} \log \frac{2A}{A+T} \right) > 0 \quad \because F_2 - F_1 > 0 \\
& \equiv \frac{1}{2A} \log \frac{A+T}{T} + \frac{1}{2T} \log \frac{A+T}{A} > 0
\end{aligned}$$

The inequality holds since $\log(x) > 0$ holds for any $x > 1$. Hence, we show $\mathcal{L}(\bar{p}_i, \bar{p}_i^*) > \mathcal{L}(\bar{p}_j, \bar{p}_j^*)$ and thus the inequality (17) hold for Case (i).

Case (ii): For Case (ii), we first show that the inequality (17) is equivalent to $\mathcal{L}(\bar{p}_i, \bar{p}_i^*) \geq \mathcal{L}(\bar{p}_j, \bar{p}_j^*)$. The inequality can be rewritten as

$$\begin{aligned}
& (|H_i| - |H_i \cap T'_i|) \times \log 2 + |H_i \cap T'_i| \times \mathcal{L}(\bar{p}_i, \bar{p}_i^*) \\
& > (|H_j| - |H_j \cap T'_j|) \times \log 2 + |H_j \cap T'_j| \times \mathcal{L}(\bar{p}_j, \bar{p}_j^*) \\
& \equiv |H_i \cap T'_i| \times (\mathcal{L}(\bar{p}_i, \bar{p}_i^*) - \log 2) > |H_j \cap T'_j| \times (\mathcal{L}(\bar{p}_j, \bar{p}_j^*) - \log 2) \\
& \equiv \frac{|H_j \cap T'_j|}{|H_i \cap T'_i|} > \frac{\log 2 - \mathcal{L}(\bar{p}_i, \bar{p}_i^*)}{\log 2 - \mathcal{L}(\bar{p}_j, \bar{p}_j^*)} \\
& \because |H_j \cap T'_j|, |H_i \cap T'_i| > 0 \text{ and } \log 2 > \mathcal{L}(\bar{p}_i, \bar{p}_i^*), \mathcal{L}(\bar{p}_j, \bar{p}_j^*).
\end{aligned}$$

By the condition of the axiom, the intersection of the target arc's head set and the reciprocal arc's tail set is larger than for e_j than for e_i , and thus $\frac{|H_j \cap T'_j|}{|H_i \cap T'_i|} > 1$ holds. Thus, Eq. (17) is implied by $\frac{\log 2 - \mathcal{L}(\bar{p}_i, \bar{p}_i^*)}{\log 2 - \mathcal{L}(\bar{p}_j, \bar{p}_j^*)} \leq 1$, which is equivalent to $\mathcal{L}(\bar{p}_i, \bar{p}_i^*) \geq \mathcal{L}(\bar{p}_j, \bar{p}_j^*)$, holds. Now we show that $\mathcal{L}(\bar{p}_i, \bar{p}_i^*) \geq \mathcal{L}(\bar{p}_j, \bar{p}_j^*)$ holds, which is rewritten as

$$\begin{aligned}
& \mathcal{L}(p_{h,i}, p_{h,i}^*) - \mathcal{L}(p_{h,j}, p_{h,j}^*) \geq 0 \\
& \equiv (F_1 - F_2) \times \ell \left(\frac{1}{T}, \frac{1}{A} \right) + (F_2 - F_1) \times \left(\frac{1}{2A} + \frac{1}{2T} \right) \log 2 \geq 0 \\
& \equiv (F_2 - F_1) \times \left(\frac{1}{2A} \log 2 + \frac{1}{2T} \log 2 - \ell \left(\frac{1}{T}, \frac{1}{A} \right) \right) \geq 0
\end{aligned}$$

Note that, unlike Case (i), where $F_1 < F_2$ holds, $F_1 \leq F_2$ holds for Case (ii). If $F_2 = F_1$, then the LHS above becomes 0, and thus above inequality holds. If $F_2 > F_1$,

$$\begin{aligned}
& (F_2 - F_1) \times \left(\frac{1}{2A} \log 2 + \frac{1}{2T} \log 2 - \ell \left(\frac{1}{T}, \frac{1}{A} \right) \right) \geq 0 \\
& \equiv \left(\frac{1}{2A} \log 2 - \frac{1}{2A} \log \frac{2T}{A+T} + \frac{1}{2T} \log 2 - \frac{1}{2T} \log \frac{2A}{A+T} \right) > 0 \quad \because F_2 - F_1 > 0 \\
& \equiv \frac{1}{2A} \log \frac{A+T}{T} + \frac{1}{2T} \log \frac{A+T}{A} > 0.
\end{aligned}$$

The inequality holds since $\log(x) > 0$ holds for any $x > 1$. Hence, we show $\mathcal{L}(\bar{p}_i, \bar{p}_i^*) \geq \mathcal{L}(\bar{p}_j, \bar{p}_j^*)$ and thus the inequality (17) hold for Case (ii). \square

Proposition 2B. HYPERREC (i.e., defining $r(e_i, R_i)$ as in Eq. (5)) satisfies Generalized Axiom 2B.

Proof. Since $|R_i| = |R_j| = 1$, the cardinality penalty terms can be ignored. The overall inequality is re-written as

$$\begin{aligned}
& r(e_i, R_i) < r(e_j, R_j) \\
& \equiv 1 - \frac{\sum_{v_i \in H_i} \mathcal{L}(p_h, p_h^*)}{|H_i| \cdot \mathcal{L}_{max}} < 1 - \frac{\sum_{v_j \in H_j} \mathcal{L}(p_h, p_h^*)}{|H_j| \cdot \mathcal{L}_{max}} \\
& \equiv \frac{\sum_{v_j \in H_j} \mathcal{L}(p_h, p_h^*)}{|H_j| \cdot \mathcal{L}_{max}} < \frac{\sum_{v_i \in H_i} \mathcal{L}(p_h, p_h^*)}{|H_i| \cdot \mathcal{L}_{max}}
\end{aligned}$$

As in the previous proof, $|H_i| = |H_j|$, and $\mathcal{L}(p_h, p_h^*)$ is identical for every $v_h \in H_k \cap T'_k$. Let $\bar{p}_k, \forall k = i, j$ be the transition probability distribution regarding the target arc e_k and its reciprocal set R_k . Here, $|H_i \cap T'_i| = |H_j \cap T'_j|$, $|T'_i| = |T'_j|$, and the number of target arc's head set nodes v_h that satisfy $\mathcal{L}(p_h, p_h^*) < \log 2$ is identical for both cases. Thus, the above inequality is re-written as

$$\begin{aligned} \frac{\sum_{v_j \in H_j} \mathcal{L}(p_h, p_h^*)}{|H_j| \cdot \mathcal{L}_{max}} &< \frac{\sum_{v_i \in H_i} \mathcal{L}(p_h, p_h^*)}{|H_i| \cdot \mathcal{L}_{max}} \\ &\equiv |H_j \cap T'_j| \times \mathcal{L}(\bar{p}_j, \bar{p}_j^*) < |H_i \cap T'_i| \times \mathcal{L}(\bar{p}_i, \bar{p}_i^*) \\ &\equiv \mathcal{L}(\bar{p}_j, \bar{p}_j^*) < \mathcal{L}(\bar{p}_i, \bar{p}_i^*). \end{aligned}$$

Now, we only need to show that the probabilistic distance between transition probability and the optimal transition probability is greater in e_i than in e_j . Let $A = |H'_i| > B = |H'_j|$. We can decompose the domain of $v \in V$ into four parts as

$$T_k \cap H'_k, \quad T_k \setminus H'_k, \quad H'_k \setminus T_k, \quad \text{and} \quad V \setminus \{H'_k \cup T_k\}, \quad \forall k = i, j$$

Here, $\text{JSD}(P \parallel Q)$ in the second and fourth parts is identical for both cases. That is, we only need to compare the probabilistic distances that are related to the first and third parts of the above four domains. That is,

$$\begin{aligned} \mathcal{L}(\bar{p}_j, \bar{p}_j^*) &< \mathcal{L}(\bar{p}_i, \bar{p}_i^*) \\ &\equiv F \times \ell\left(\frac{1}{B}, \frac{1}{T}\right) + \frac{B-F}{2B} \log 2 < F \times \ell\left(\frac{1}{A}, \frac{1}{T}\right) + \frac{A-F}{2A} \log 2, \end{aligned}$$

where $F = |H'_i \cap T_i| = |H'_j \cap T_j|$ and $T = |T_i| = |T_j|$. Note that $A > B$. Overall inequality is rewritten as

$$\begin{aligned} \mathcal{L}(\bar{p}_j, \bar{p}_j^*) &< \mathcal{L}(\bar{p}_i, \bar{p}_i^*) \\ &\equiv \frac{F}{2} \left(\frac{1}{B} - \frac{1}{A}\right) \log 2 > F \times \left(\ell\left(\frac{1}{B}, \frac{1}{T}\right) - \ell\left(\frac{1}{A}, \frac{1}{T}\right)\right) \end{aligned}$$

To simplify the equation, we unfold $\ell(p, q)$ as

$$\begin{aligned} \frac{F}{2} \left(\frac{1}{B} - \frac{1}{A}\right) \log 2 &> F \times \left(\ell\left(\frac{1}{B}, \frac{1}{T}\right) - \ell\left(\frac{1}{A}, \frac{1}{T}\right)\right) \\ &\equiv \frac{1}{2} \left(\frac{1}{B} - \frac{1}{A}\right) \log 2 > \frac{1}{2T} \log \frac{2B}{B+T} + \frac{1}{2B} \log \frac{2T}{B+T} - \frac{1}{2T} \log \frac{2A}{A+T} - \frac{1}{2A} \log \frac{2T}{A+T} \\ &\equiv \left(\frac{1}{B} - \frac{1}{A}\right) \log 2 > \frac{1}{T} \log \frac{2B}{B+T} + \frac{1}{B} \log \frac{2T}{B+T} - \frac{1}{T} \log \frac{2A}{A+T} - \frac{1}{A} \log \frac{2T}{A+T} \\ &\equiv 0 > \frac{1}{T} \log \frac{B}{B+T} + \frac{1}{B} \log \frac{T}{B+T} - \frac{1}{T} \log \frac{A}{A+T} - \frac{1}{A} \log \frac{T}{A+T} \\ &\because \text{pull 2 inside each log term out} \\ &\equiv 0 > \frac{1}{T} \log \frac{B(A+T)}{A(B+T)} - \frac{1}{B} \log \frac{B+T}{T} + \frac{1}{A} \log \frac{A+T}{T} \\ &\equiv 0 > \log \frac{AB+BT}{AB+AT} + \frac{T}{A} \log \left(1 + \frac{A}{T}\right) - \frac{T}{B} \log \left(1 + \frac{B}{T}\right) \quad \because \text{multiply both sides by } T \end{aligned}$$

We show that the last inequality holds by splitting it into two parts: $\log \frac{AB+BT}{AB+AT} < 0$ and $\frac{T}{A} \log \left(1 + \frac{A}{T}\right) - \frac{T}{B} \log \left(1 + \frac{B}{T}\right) < 0$. The first part is trivial since $B < A$ implies

$$\frac{AB+BT}{AB+AT} < 1.$$

In the second part, each term is in the form of $f(x) = \frac{1}{x} \log(1+x)$. Since $f(x)$ is decreasing at $x > 0$,⁶ $A > B$ implies

$$\frac{T}{A} \log \left(1 + \frac{A}{T}\right) - \frac{T}{B} \log \left(1 + \frac{B}{T}\right) < 0.$$

□

⁶Note that $(1 + \frac{1}{x})^x$ is a well-known increasing function whose limit as $x \rightarrow \infty$ is e . Thus, $\log(1 + \frac{1}{x})^x = x \log(1 + \frac{1}{x})$ is also an increasing function, and since $x' = 1/x$ is decreasing at $x > 0$, $x' \log(1 + \frac{1}{x'}) = \frac{1}{x} \log(1 + \frac{1}{x})$ is decreasing at $x > 0$.

A.2.3 Proof of the Fact that HyperRec Satisfies Axiom 3

Through an example, **Axiom 3** states that when two arcs inversely overlap equally with their reciprocal sets, an arc with a single reciprocal arc is more reciprocal than one with multiple reciprocal arcs. **Axiom 3** is split into two cases and each case is formalized in **Generalized Axioms 3A** and **3B** respectively, where an arc with a single reciprocal arc and an arc with exactly two reciprocal arcs are compared. In **Remark 1**, we further generalize them to encompass a comparison of the former and an arc with two or more reciprocal arcs and provide a proof sketch to show that these extended statements hold true for our proposed measure.

Proposition 3A. HYPERREC (i.e., defining $r(e_i, R_i)$ as in Eq. (5)) satisfies Generalized Axiom 3A.

Proof. Since the sizes of the reciprocal sets differ, the cardinality penalty term should be considered. Here, $r(e_i, R_i)$ and $r(e_j, R_j)$ is rewritten as

$$r(e_i, R_i) = \left(\frac{1}{2}\right)^\alpha \left(1 - \frac{\sum_{v_h \in H_i} \mathcal{L}(p_h, p_h^*)}{|H_i| \cdot \mathcal{L}_{max}}\right),$$

$$r(e_j, R_j) = \left(1 - \frac{\sum_{v_h \in H_j} \mathcal{L}(p_h, p_h^*)}{|H_j| \cdot \mathcal{L}_{max}}\right).$$

Since $\alpha > 0$, $r(e_i, R_i) < r(e_j, R_j)$ is implied by

$$\left(1 - \frac{\sum_{v_h \in H_i} \mathcal{L}(p_h, p_h^*)}{|H_i| \cdot \mathcal{L}_{max}}\right) \leq \left(1 - \frac{\sum_{v_h \in H_j} \mathcal{L}(p_h, p_h^*)}{|H_j| \cdot \mathcal{L}_{max}}\right).$$

Since $|H_i| = |H_j|$, the inequality is rewritten as

$$\begin{aligned} \left(1 - \frac{\sum_{v_h \in H_i} \mathcal{L}(p_h, p_h^*)}{|H_i| \cdot \mathcal{L}_{max}}\right) &\leq \left(1 - \frac{\sum_{v_h \in H_j} \mathcal{L}(p_h, p_h^*)}{|H_j| \cdot \mathcal{L}_{max}}\right) \\ &\equiv \frac{\sum_{v_h \in H_j} \mathcal{L}(p_h, p_h^*)}{|H_j| \cdot \mathcal{L}_{max}} \leq \frac{\sum_{v_h \in H_i} \mathcal{L}(p_h, p_h^*)}{|H_i| \cdot \mathcal{L}_{max}} \\ &\equiv \sum_{v_h \in H_j} \mathcal{L}(p_h, p_h^*) \leq \sum_{v_h \in H_i} \mathcal{L}(p_h, p_h^*). \end{aligned} \quad (18)$$

For the target arc e_i , since $T'_{i1} = T'_{i2}$, p_h for every $v_h \in H_i$ has the same distribution. For the target arc e_j , since there is only one single reciprocal arc, p_h for every $v_h \in H_i$ has the same distribution. Let $\bar{p}_k, \forall k = i, j$ be the transition probability distribution regarding the target arc e_k and its reciprocal set R_k . Here, the inequality (18) is rewritten as

$$\begin{aligned} \sum_{v_h \in H_j} \mathcal{L}(p_h, p_h^*) &\leq \sum_{v_h \in H_i} \mathcal{L}(p_h, p_h^*) \\ &\equiv |H_j \cap T'_j| \times \mathcal{L}(\bar{p}_j, \bar{p}_j^*) \leq |H_i \cap T'_{i1}| \times \mathcal{L}(\bar{p}_i, \bar{p}_i^*) \end{aligned}$$

Since $e'_{i1} \subseteq_{(R)} e_i$, $e'_{i2} \subseteq_{(R)} e_i$, $e'_j \subseteq_{(R)} e_j$, and $|T'_j| = |T'_{i1}|$, the last inequality is rewritten as

$$\begin{aligned} |H_j \cap T'_j| \times \mathcal{L}(\bar{p}_j, \bar{p}_j^*) &\leq |H_i \cap T'_{i1}| \times \mathcal{L}(\bar{p}_i, \bar{p}_i^*) \\ &\equiv |T'_j| \times \mathcal{L}(\bar{p}_j, \bar{p}_j^*) \leq |T'_{i1}| \times \mathcal{L}(\bar{p}_i, \bar{p}_i^*) \\ &\equiv \mathcal{L}(\bar{p}_j, \bar{p}_j^*) \leq \mathcal{L}(\bar{p}_i, \bar{p}_i^*). \end{aligned}$$

The proof can be done by showing the last inequality, $\mathcal{L}(\bar{p}_j, \bar{p}_j^*) \leq \mathcal{L}(\bar{p}_i, \bar{p}_i^*)$.

In order to show $\mathcal{L}(\bar{p}_j, \bar{p}_j^*) \leq \mathcal{L}(\bar{p}_i, \bar{p}_i^*)$, we should take a close look at the transition probability in e_i . Since the head sets of the two reciprocal arcs do not overlap, the transition probability is

$$p_{h,i}(v) = \begin{cases} \frac{1}{2|H'_{i1}|} & \text{if } v \in H'_{i1} \\ \frac{1}{2|H'_{i2}|} & \text{if } v \in H'_{i2} \\ 0 & \text{otherwise.} \end{cases}$$

Since $e'_{i1} \subseteq_{(R)} e_i$, $e'_{i2} \subseteq_{(R)} e_i$, and $e'_j \subseteq_{(R)} e_j$, the domain of $v \in V$ can be divided into

$$\begin{aligned} &H'_{i1}, \quad H'_{i2}, \quad T_i \setminus \{H'_{i1} \cup H'_{i2}\}, \quad \text{and } V \setminus T_i, \quad \text{for } e_i, \\ &H'_j, \quad T_j \setminus H'_j, \quad \text{and } V \setminus T_j, \quad \text{for } e_j. \end{aligned}$$

Since $|T_i| = |T_j|$, the probability mass for the last part is identical for both cases. Let $A = |H_j|$, $B = |H_{i1}|$, and $T = |T_i| = |T_j|$. Since $H'_{i1}, H'_{i2} \subseteq T_i$, $H'_j \subseteq T_j$, $H'_{i1} \cap H'_{i2} = \emptyset$, and $|(H'_{i1} \cup H'_{i2}) \cap T_i| = |H'_j \cap T_j|$, $|H_{i1}| + |H_{i2}| = |H_j|$ holds. Then, based on the above fact, we rewrite $\mathcal{L}(\bar{p}_j, \bar{p}_j^*) \leq \mathcal{L}(\bar{p}_i, \bar{p}_i^*)$ as

$$\begin{aligned}
\mathcal{L}(\bar{p}_j, \bar{p}_j^*) &\leq \mathcal{L}(\bar{p}_i, \bar{p}_i^*) \\
&\equiv A \times \ell\left(\frac{1}{T}, \frac{1}{A}\right) + \frac{T-A}{2T} \log 2 \\
&\leq B \times \ell\left(\frac{1}{T}, \frac{1}{2B}\right) + (A-B) \times \ell\left(\frac{1}{T}, \frac{1}{2(A-B)}\right) + \frac{T-B-(A-B)}{2T} \log 2 \\
&\equiv A \times \ell\left(\frac{1}{T}, \frac{1}{A}\right) \leq B \times \ell\left(\frac{1}{T}, \frac{1}{2B}\right) + (A-B) \times \ell\left(\frac{1}{T}, \frac{1}{2(A-B)}\right) \tag{19} \\
&\equiv \frac{A}{2T} \log \frac{2A}{A+T} + \frac{A}{2A} \log \frac{2T}{A+T} \\
&\leq \frac{B}{2T} \log \frac{4B}{2B+T} + \frac{B}{4B} \log \frac{2T}{2B+T} \\
&+ \frac{(A-B)}{2T} \log \frac{4(A-B)}{2(A-B)+T} + \frac{(A-B)}{4(A-B)} \log \frac{2T}{2(A-B)+T}, \quad \because \text{unfold } \ell(p, q) \\
&\equiv \frac{A}{2T} \log \frac{A}{A+T} + \frac{A}{2A} \log \frac{T}{A+T} \\
&\leq \frac{B}{2T} \log \frac{2B}{2B+T} + \frac{B}{4B} \log \frac{T}{2B+T} \\
&+ \frac{(A-B)}{2T} \log \frac{2(A-B)}{2(A-B)+T} + \frac{(A-B)}{4(A-B)} \log \frac{T}{2(A-B)+T},
\end{aligned}$$

where, for the last equivalence, we subtract $(\frac{A}{2T} + \frac{1}{2}) \log 2 = (\frac{A}{2T} + \frac{A}{2A}) \log 2 = (\frac{B}{2T} + \frac{B}{4B} + \frac{A-B}{2T} + \frac{B-A}{4(B-A)}) \log 2$ from both sides. We show the last inequality by dividing it into two and proving each. If the following two inequality holds, the proof is done.

$$\frac{A}{2T} \log \frac{A}{A+T} \leq \frac{B}{2T} \log \frac{2B}{2B+T} + \frac{(A-B)}{2T} \log \frac{2(A-B)}{2(A-B)+T}, \tag{20}$$

$$\frac{1}{2} \log \frac{T}{A+T} \leq \frac{1}{4} \log \frac{T}{2B+T} + \frac{1}{4} \log \frac{T}{2(A-B)+T}. \tag{21}$$

We first show the inequality (20). By multiplying by $2T$ both sides, we get

$$\begin{aligned}
\frac{A}{2T} \log \frac{A}{A+T} &\leq \frac{B}{2T} \log \frac{2B}{2B+T} + \frac{(A-B)}{2T} \log \frac{2(A-B)}{2(A-B)+T} \\
&\equiv A \log \frac{A}{A+T} \leq B \log \frac{2B}{2B+T} + (A-B) \log \frac{2(A-B)}{2(A-B)+T} \tag{22}
\end{aligned}$$

Here, we prove this inequality by using the functional form of $f(B) = B \log \frac{2B}{2B+T} + (A-B) \log \frac{2(A-B)}{2(A-B)+T}$ where $0 < B < A$. Its derivative is

$$\begin{aligned}
\frac{\partial f(B)}{\partial B} &= \log(2B) - \log(2B+T) + B \left(\frac{2}{2B} - \frac{2}{2B+T} \right) \\
&\quad - \log(2(A-B)) + \log(2(A-B)+T) - (A-B) \left(\frac{2}{2(A-B)} - \frac{2}{2(A-B)+T} \right). \\
&= \log(2B) - \log(2B+T) - \frac{2B}{2B+T} \\
&\quad - \log(2(A-B)) + \log(2(A-B)+T) + \frac{2(A-B)}{2(A-B)+T} \\
&= \log \frac{2B}{2B+T} - \frac{2B}{2B+T} - \log \frac{2(A-B)}{2(A-B)+T} + \frac{2(A-B)}{2(A-B)+T}.
\end{aligned}$$

Thus, $\frac{\partial f(B)}{\partial B} = \log x - x - (\log y - y)$ for $x = \frac{2B}{2B+T}$ and $y = \frac{2(A-B)}{2(A-B)+T}$, which satisfy $0 < x, y < 1$, and it has the following properties:

- If we plug in $B = \frac{A}{2}$, $f'(B) = 0$ holds,

- $\log x - x$ is an increasing function at $0 < x < 1$,
- If $0 < B < \frac{A}{2}$, then $(\log y) - y > (\log x) - x$, which implies $f'(B) < 0$,
- If $\frac{A}{2} < B < A$, then $(\log x) - x > (\log y) - y$, which implies $f'(B) > 0$.

From these properties, we can derive

$$f'(B) \begin{cases} < 0 & \text{if } 0 < B < \frac{A}{2} \\ = 0 & \text{if } B = \frac{A}{2} \\ > 0 & \text{if } \frac{A}{2} < B < A. \end{cases}$$

Hence, when $0 < B < A$, $f(B)$ has its minimum value at $B = A/2$, and therefore the inequality (22), which is equivalent to the inequality (20), holds. Now we show the inequality (21), which is rewritten as

$$\begin{aligned} \frac{1}{2} \log \frac{T}{A+T} &\leq \frac{1}{4} \log \frac{T}{2B+T} + \frac{1}{4} \log \frac{T}{2(A-B)+T} \\ &\equiv \frac{1}{4} \log \frac{T^2}{(A+T)(A+T)} \leq \frac{1}{4} \log \frac{T^2}{(2B+T)(2(A-B)+T)}, \\ &\equiv (2B+T)(2(A-B)+T) \leq (A+T)(A+T) \\ &= 4B(A-B) + 2AT + T^2 \leq A^2 + 2AT + T^2 \\ &\equiv A^2 - 4AB + 4B^2 = (A-2B)^2 \geq 0. \end{aligned}$$

The last inequality trivially holds. \square

Proposition 3B. HYPERREC (i.e., defining $r(e_i, R_i)$ as in Eq. (5)) satisfies Generalized Axiom 3B.

Proof. By following the proof of Proposition 3A, we can show that $r(e_i, R_i) < r(e_j, R_j)$ is implied by

$$\sum_{v_h \in H_i} \mathcal{L}(p_h, p_h^*) \leq \sum_{v_h \in H_j} \mathcal{L}(p_h, p_h^*).$$

Since $T'_{i1} \cap T'_{i2} = \emptyset$ and $H'_{i1} = H'_{i2}$, the transition probability for every $v_h \in H_i \cap \{T'_{i1} \cup T'_{i2}\}$ is identical for e_i . This is also true for e_j , whose reciprocal set has only one arc. Let $\bar{p}_k, \forall k = i, j$ be the transition probability distribution regarding the target arc e_k and its reciprocal set R_k . Since $|H_i \cap \{T'_{i1} \cup T'_{i2}\}| = |H_j \cap T'_j|$, the above inequality is rewritten as

$$\mathcal{L}(\bar{p}_i, \bar{p}_i^*) \leq \mathcal{L}(\bar{p}_j, \bar{p}_j^*).$$

Since $e'_{i1} \subseteq_{(R)} e_i$, $e'_{i2} \subseteq_{(R)} e_i$, $e'_j \subseteq_{(R)} e_j$, and $|H'_{i1}| = |H'_j|$, the probabilistic distances for e_i and e_j are identical. That is,

$$\mathcal{L}(\bar{p}_i, \bar{p}_i^*) = \mathcal{L}(\bar{p}_j, \bar{p}_j^*), \quad (23)$$

and thus $\mathcal{L}(\bar{p}_i, \bar{p}_i^*) \leq \mathcal{L}(\bar{p}_j, \bar{p}_j^*)$ also holds. \square

Remark 1 (Extension of Propositions 3A and 3B to Multiple Hyperarc Cases). *Although the statement of Proposition 3A presents a case with a single arc in R_i and two arcs in R_j , it can be further generalized: a single arc in R_i and $K \geq 2$ hyperarcs in R_j under the following conditions, which are equivalent to the current conditions for $K = 2$: (1) the head sets of the arcs in R_i are disjoint and their tail sets are identical, (2) all arcs in R_i satisfy the condition of $\subseteq_{(R)}$, and (3) the coverage of T_i by the head sets of the arcs in R_i is of the same size as the coverage of T_j by the head set of the arc in R_j .*

We provide a proof sketch to demonstrate the validity of HYPERREC in this generalized setting. As in the proof of Proposition 3A, it suffices to show that Eq. (24) holds, which generalizes Eq. (19),

$$A \times \ell \left(\frac{1}{T}, \frac{1}{A} \right) \leq B_1 \ell \left(\frac{1}{T}, \frac{1}{KB_1} \right) + \dots + B_K \ell \left(\frac{1}{T}, \frac{1}{KB_K} \right), \quad (24)$$

where $A = \sum_{i=1}^K B_i$. *Considering that the Jensen-Shannon Divergence (JSD) is an average of two KL-divergence terms, which is a well-known convex function when one probability distribution is fixed ($1/T$ in our case), we can derive that each term ℓ in Eq. (24) is also a convex function.*

From this fact, we can apply Jensen's Inequality, which states: $f(a_1x_1 + \dots + a_Kx_K) \leq a_1f(x_1) + \dots + a_Kf(x_K)$ holds for a convex function f and non-negative coefficients a_1, \dots, a_K where $\sum_{i=1}^K a_i = 1$.

By considering the fact that $\ell(\frac{1}{T}, x)$ is a convex function with respect to x , we derive Eq. (25) by setting $a_i = B_i/A$ and $x_i = 1/(KB_i)$.

$$\begin{aligned} \ell\left(\frac{1}{T}, \frac{1}{A}\right) &= \ell\left(\frac{1}{T}, \frac{K}{AK}\right) = \ell\left(\frac{1}{T}, \frac{1}{KB_1} \times \frac{B_1}{A} + \dots + \frac{1}{KB_K} \times \frac{B_K}{A}\right) \\ &\leq \frac{B_1}{A} \ell\left(\frac{1}{T}, \frac{1}{KB_1}\right) + \dots + \frac{B_K}{A} \ell\left(\frac{1}{T}, \frac{1}{KB_K}\right). \end{aligned} \quad (25)$$

Multiplying both sides of Eq. (25) by A implies Eq. (24), which is the result we aim to show.

Similarly, we can further generalize **Proposition 3B** to case with a single arc in R_i and $K \geq 2$ arcs in R_j under the following conditions, which are equivalent to the current conditions when $K = 2$: (1) the tail sets of the arcs in R_i are disjoint and their head sets are identical, (2) all arcs in R_i satisfy the condition of $\subseteq_{(R)}$, and (3) the coverage of H_i by the tail sets of the arcs in R_i is of the same size as the coverage of H_j by the tail set of the arc in R_j . The proof provided for **Proposition 3B** can be directly applied in this generalized setting to show the validity of **HYPERREC**.

A.2.4 Proof of the Fact that HyperRec Satisfies Axiom 4

Through an example, **Axiom 4** states that an arc whose reciprocal arcs are **equally** reciprocal to all nodes in the arc is more reciprocal than one with reciprocal arcs **biased** towards a subset of nodes in the arc. The generalized statement of **Axiom 4** is formalized in **Generalized Axiom 4**.

Proposition 4. **HYPERREC** (i.e., defining $r(e_i, R_i)$ as in Eq. (5)) satisfies Generalized Axiom 4.

Proof. By the definition, the inequality is rewritten as

$$\begin{aligned} r(e_i, R_i) &< r(e_j, R_j) \\ &= \left(\frac{1}{|R_i|}\right)^\alpha \left(1 - \frac{\sum_{v_h \in H_i} \mathcal{L}(p_h, p_h^*)}{|H_i| \cdot \mathcal{L}_{max}}\right) < \left(\frac{1}{|R_j|}\right)^\alpha \left(1 - \frac{\sum_{v_h \in H_j} \mathcal{L}(p_h, p_h^*)}{|H_j| \cdot \mathcal{L}_{max}}\right). \end{aligned}$$

Let $\bar{p}_k, \forall k = i, j$ be the transition probability distribution regarding the target arc e_k and its reciprocal set R_k which does not rely on the starting node v_h . The above inequality is rewritten as

$$\begin{aligned} r(e_i, R_i) &< r(e_j, R_j) \\ &\equiv \left(1 - \frac{\sum_{v_h \in H_i} \mathcal{L}(p_h, p_h^*)}{|H_i| \cdot \mathcal{L}_{max}}\right) < \left(1 - \frac{\sum_{v_h \in H_j} \mathcal{L}(p_h, p_h^*)}{|H_j| \cdot \mathcal{L}_{max}}\right) \quad \because |R_i| = |R_j| \\ &\equiv \sum_{v_h \in H_j} \mathcal{L}(p_h, p_h^*) < \sum_{v_h \in H_i} \mathcal{L}(p_h, p_h^*) \quad \because |H_i| = |H_j| \\ &\equiv \mathcal{L}(\bar{p}_j, \bar{p}_j^*) < \mathcal{L}(\bar{p}_i, \bar{p}_i^*) \quad \because T_i' = H_i \text{ and } T_j' = H_j \end{aligned}$$

Here, we prove the last inequality by showing that, in the above setting, (a) R_j minimizes the distance (i.e., $\mathcal{L}(p_{h,j}, p_{h,j}^*) \equiv \mathcal{L}(\bar{p}_j, \bar{p}_j^*)$), and (b) the distance is inevitably larger in all other cases. By the assumptions, for the target arc e_j , the corresponding reciprocal arcs have a head set of size 2, and the number of reciprocal arcs equals the number of tail nodes (i.e., $|R_j| = |T_j|$). In addition, the head set of every reciprocal arc is a subset of the tail set T_j of e_j and $T_j' = H_j$. Thus, Eq. (3), which is about e_j , implies that every node $v \in T_j$ in the tail set is included in two of the head sets of the reciprocal arcs. Because of these facts, the transition probability can be written as

$$p_{h,j}(v) = \begin{cases} \frac{1}{2|T_j|} + \frac{1}{2|T_j|} = \frac{1}{|T_j|} & \text{if } v \in T_j, \\ 0 & \text{otherwise,} \end{cases}$$

Note that this is identical to the optimal transition probability.

Now, consider the case of e_i . Here, due to Eq. (2), the transition probability cannot be uniform as in the case of e_j . Assume a node $v'_{i1} \in T_i$ belongs to reciprocal arcs' head sets $K \neq 2$ times. Then, the transition probability assigned to v'_{i1} is $p(v'_{i1}) = \frac{1}{2|T_i|} \times K \neq \frac{1}{|T_i|}$. This result indicates that the transition probability of e_i is not the only optimal one. Thus, the following inequality holds:

$$\mathcal{L}(\bar{p}_j, \bar{p}_j^*) < \mathcal{L}(\bar{p}_i, \bar{p}_i^*)$$

□

A.2.5 Proof of the Fact that HyperRec Satisfies Axioms 5-8

Proposition 5. HYPERREC (i.e., defining $r(e_i, R_i)$ as in Eq. (5)) satisfies **Axiom 5**.

Proof. This can be shown by using the known range of the probabilistic distance $\mathcal{L}(p, q)$ as follows:

$$\begin{aligned}
0 &\leq \sum_{v_h \in H_i} \frac{\mathcal{L}(p_h, p_h^*)}{\mathcal{L}_{max}} \leq |H_i| \quad (\because 0 \leq \mathcal{L}(p, q) \leq \mathcal{L}_{max}, \forall p, q) \\
&\equiv 0 \leq \frac{\sum_{v_h \in H_i} \mathcal{L}(p_h, p_h^*)}{|H_i| \cdot \mathcal{L}_{max}} \leq 1 \\
&\equiv 0 \leq 1 - \frac{\sum_{v_h \in H_i} \mathcal{L}(p_h, p_h^*)}{|H_i| \cdot \mathcal{L}_{max}} \leq 1 \\
&\equiv 0 \leq \left(\frac{1}{|R_i|}\right)^\alpha \left(1 - \frac{\sum_{v_h \in H_i} \mathcal{L}(p_h, p_h^*)}{|H_i| \cdot \mathcal{L}_{max}}\right) \leq 1 \quad (\because \alpha > 0)
\end{aligned}$$

□

Proposition 6. HYPERREC (i.e., defining $r(G)$ as in Eq. (1)) satisfies **Axiom 6**.

Proof. Recall that the hypergraph level reciprocity of HYPERREC is defined as

$$r(G) = \frac{1}{|E|} \sum_{i=1}^{|E|} r(e_i, R_i)$$

By the assumption, the size of every arc's head set is 1, and thus each $r(e_i, R_i)$ is rewritten as

$$r(e_i) = \max_{R_i \subseteq E, R_i \neq \emptyset} \left(\frac{1}{|R_i|}\right)^\alpha \left(1 - \frac{\mathcal{L}(p_h, p_h^*)}{\mathcal{L}_{max}}\right),$$

where $\{v_h\} = H_i$. Here, the optimal transition probability is

$$p_h^*(v) = \begin{cases} 1 & \text{if } \{v\} = T_i, \\ 0 & \text{otherwise.} \end{cases}$$

For a case where the perfectly reciprocal opponent $e'_i = \langle H'_i = T_i, T'_i = H_i \rangle$ of e_i exists (i.e., $e'_i \in E$), $R_i = \{e'_i\}$ maximizes $\left(\frac{1}{|R_i|}\right)^\alpha \left(1 - \frac{\mathcal{L}(p_h, p_h^*)}{\mathcal{L}_{max}}\right)$ since it minimizes both $|R_i|$ (to 1) and $\mathcal{L}(p_h, p_h^*)$ (to 0). Thus, $r(e_i)$ becomes 1.

For a case where the perfectly reciprocal opponent $e'_i = \langle H'_i = T_i, T'_i = H_i \rangle$ of e_i does not exist (i.e., $e'_i \notin E$). Then, for each arc e_k in the reciprocal set R_i , since $|H_i| = |T_i| = |H_k| = |T_k| = 1$, $H_i \cap T_k = \emptyset$ or $T_i \cap H_k = \emptyset$ should hold. Thus, there is no transition possibility from any node in $\in H_i$ to any node in T_i , and as a result, $p_h(v) = 0, \forall v_h \in H_i, \forall v \in T_i$. Hence, for every $R_i \subseteq E$, by **A-II**, $\mathcal{L}(p_h, p_h^*) = \mathcal{L}_{max}$, and thus $r(e_i) = 0$.

If we consider both cases together, $r(e_i)$ becomes an indicator function that gives 1, if there exists the perfectly reciprocal opponent, and 0, otherwise. Formally,

$$\begin{aligned}
r(G) &= \frac{1}{|E|} \sum_{i=1}^{|E|} r(e_i) \\
&= \frac{1}{|E|} \sum_{i=1}^{|E|} \mathbb{1}(\exists e'_i \in E \text{ such that } H'_i = T_i \text{ and } T'_i = H_i),
\end{aligned}$$

where $\mathbb{1}(\text{TRUE}) = 1$ and $\mathbb{1}(\text{FALSE}) = 0$; and this is identical to the digraph reciprocity measure [Newman et al., 2002, Garlaschelli and Loffredo, 2004], i.e., $|E^{\leftrightarrow}|/|E|$. □

Proposition 7. HYPERREC (i.e., defining $r(G)$ as in Eq. (1)) satisfies **Axiom 7**.

Proof. Recall that the hypergraph-level reciprocity of HYPERREC is defined as

$$r(G) = \frac{1}{|E|} \sum_{i=1}^{|E|} r(e_i) = \frac{1}{|E|} \sum_{i=1}^{|E|} \max_{R_i \subseteq E, R_i \neq \emptyset} r(e_i, R_i)$$

By **Axiom 5**, $0 \leq r(e_i, R_i) \leq 1$ for any e_i and R_i . This implies $0 \leq \sum_{i=1}^{|E|} r(e_i) \leq |E|$, which is equivalent to $0 \leq r(G) = \frac{1}{|E|} \sum_{i=1}^{|E|} r(e_i) \leq 1$. □

Proposition 8. HYPERREC (i.e., defining $r(G)$ as in Eq. (1)) satisfies **Axiom 8**.

Proof. We first show that the maximum value of HYPERREC is attainable under the given condition of **Axiom 8**. From an arbitrary hypergraph G , let $E' = \{e_i \in E : \langle T_i, H_i \rangle \notin E\}$ be the set of arcs whose perfectly reciprocal opponents do not exist in G . Let $E^{add} = \bigcup_{e_{ki} \in E'} \langle T_i, H_i \rangle$ be the set of perfectly reciprocal opponents of the arcs in E' . If we add E^{add} to G , which gives $G^+ = (V, E^+ = E \cup E^{add})$, then for each arc $e_i \in E^+$, the perfectly reciprocal opponent $e'_i = \langle H'_i = T_i, T'_i = H_i \rangle$ of e_i exists (i.e., $e'_i \in E^+$), and thus

$$\begin{aligned} r(e_i) &= r(e_i, \{e'_i\}) = \left(1 - \frac{\sum_{v_h \in H_i} \mathcal{L}(p_h, p_h^*)}{|H_i| \cdot \mathcal{L}_{max}}\right) \\ &= \left(1 - \frac{0 + \dots + 0}{|H_i| \cdot \mathcal{L}_{max}}\right) \quad (\because p_h = p_h^*) \\ &= 1, \end{aligned}$$

which implies that $r(G^+) = \frac{1}{|E^+|} \sum_{i=1}^{|E^+|} r(e_i) = 1$.

We now show that the minimum value of HYPERREC is attainable under the given condition of **Axiom 8**. From an arbitrary hypergraph $G = (V, E)$, let $E^- = \{e_i\}$ be a hyperarc set that contains any single hyperarc $e_i \in E$. For a hypergraph $G^- = (V, E^-)$, the only possible choice of R_i is $R_i = \{e_i\}$ since R_i should be a non-empty set and there exists only a single hyperarc e_i in G^- , and thus

$$\begin{aligned} r(e_i) &= r(e_i, \{e_i\}) = \left(1 - \frac{\sum_{v_h \in H_i} \mathcal{L}(p_h, p_h^*)}{|H_i| \cdot \mathcal{L}_{max}}\right) \\ &= \left(1 - \frac{|H_i| \cdot \mathcal{L}_{max}}{|H_i| \cdot \mathcal{L}_{max}}\right) \quad (\because \mathbf{A-IV} \text{ and } \mathbf{A-V}) \\ &= 0, \end{aligned}$$

which implies that $r(G^-) = r(e_i) = 0$. □

A.3 Proof of Theorem 2

Proof. Refer to Section 3.4 for the definition of $\Phi_i(\langle H'_i, T'_i \rangle)$. Given a target arc e_i , let e_a and e_b be two arcs in a set $\Phi_i(\langle H'_i, T'_i \rangle)$ where $A = |H_a| \leq B = |H_b|$. Consider an arbitrary reciprocal set $R_i \subseteq E$. We use $p_{(i,a,h)}$ to denote the probability distribution at each node $v_h \in H'_i$ when the reciprocal set is $R_i \cup \{e_a\}$. Then, probabilistic distance between $p_{(i,a,h)}$ and p_h^* is rewritten as

$$\begin{aligned} \mathcal{L}(p_{(i,a,h)}, p_h^*) &= \sum_{v \in T'_i} \ell\left(\frac{1}{|T'_i|}, \frac{Kq_{(i,h)}(v)}{K+1} + \frac{1}{A(K+1)}\right) + \sum_{v \in T_i \setminus T'_i} \ell\left(\frac{1}{|T'_i|}, \frac{Kq_{(i,h)}(v)}{K+1}\right) \\ &\quad + \sum_{v \in (\bigcup_{e_k \in E'_{(i,h)}} H_k) \setminus T_i} \frac{Kq_{(i,h)}(v)}{2(K+1)} \log 2 + \sum_{v \in H_a \setminus T_i} \frac{1}{2A(K+1)} \log 2, \quad (26) \end{aligned}$$

where $E'_{(i,h)} = \{e_k \in R_i : v_h \in T_k\}$, $K = |E'_{(i,h)}|$, and $q_{(i,h)}$ is the probability distribution at each node $v_h \in H'_i$ when the reciprocal set is R_i . It should be noticed that the definition of H'_i and T'_i , $H'_i = T_a \cap H_i = T_b \cap H_i$ and $T'_i = H_a \cap T_i = H_b \cap T_i$ hold. In the same way, we define $p_{(i,b,h)}$ is as the probabilistic distribution at each node $v_h \in H'_i$ when $R_i \cup \{e_b\}$ is the reciprocal set. Then, $\mathcal{L}(p_{(i,b,h)}, p_h^*)$ can be rewritten as in Eq. (26).

We prove the theorem by showing that $\mathcal{L}(p_{(i,a,h)}, p_h^*) \leq \mathcal{L}(p_{(i,b,h)}, p_h^*)$ holds for every $v_h \in H'_i = H_i \cap T_a = H_i \cap T_b$. Note that the second and third terms of the RHS do not depend on e_a and e_b , and they are identical in $\mathcal{L}(p_{(i,a,h)}, p_h^*)$ and $\mathcal{L}(p_{(i,b,h)}, p_h^*)$. Thus, we rewrite $\mathcal{L}(p_{(i,a,h)}, p_h^*) \leq \mathcal{L}(p_{(i,b,h)}, p_h^*)$ as

$$\begin{aligned} \mathcal{L}(p_{(i,a,h)}, p_h^*) &\leq \mathcal{L}(p_{(i,b,h)}, p_h^*) \\ &\equiv \sum_{v \in T'_i} \ell\left(\frac{1}{|T'_i|}, \frac{Kq_{(i,h)}(v)}{K+1} + \frac{1}{A(K+1)}\right) + \sum_{v \in H_a \setminus T_i} \frac{1}{2A(K+1)} \log 2 \\ &\leq \sum_{v \in T'_i} \ell\left(\frac{1}{|T'_i|}, \frac{Kq_{(i,h)}(v)}{K+1} + \frac{1}{B(K+1)}\right) + \sum_{v \in H_b \setminus T_i} \frac{1}{2B(K+1)} \log 2. \end{aligned}$$

For simplicity, let $|T_i| = T$ and $|T'_i| = F$. Then, the above inequality is rewritten as

$$\begin{aligned} & \sum_{v \in T'_i} \ell\left(\frac{1}{T}, \frac{Kq_{(i,h)}(v)}{K+1} + \frac{1}{A(K+1)}\right) - \ell\left(\frac{1}{T}, \frac{Kq_{(i,h)}(v)}{K+1} + \frac{1}{B(K+1)}\right) \\ & \leq \frac{B-F}{2B(K+1)} \log 2 - \frac{A-F}{2A(K+1)} \log 2. \end{aligned} \quad (27)$$

Let $v' = \operatorname{argmax}_{v \in T'_i} \ell\left(\frac{1}{T}, \frac{Kq_{(i,h)}(v)}{K+1} + \frac{1}{A(K+1)}\right) - \ell\left(\frac{1}{T}, \frac{Kq_{(i,h)}(v)}{K+1} + \frac{1}{B(K+1)}\right)$, and let $p' = q_{(i,h)}(v')$. Then, the following inequality holds:

$$\begin{aligned} & \sum_{v \in T'_i} \ell\left(\frac{1}{T}, \frac{Kq_{(i,h)}(v)}{K+1} + \frac{1}{A(K+1)}\right) - \ell\left(\frac{1}{T}, \frac{Kq_{(i,h)}(v)}{K+1} + \frac{1}{B(K+1)}\right) \\ & \leq F \times \left(\ell\left(\frac{1}{T}, \frac{Kp'}{K+1} + \frac{1}{A(K+1)}\right) - \ell\left(\frac{1}{T}, \frac{Kp'}{K+1} + \frac{1}{B(K+1)}\right) \right) \end{aligned}$$

Thus, the inequality (27) is implied by

$$\begin{aligned} & F \times \left(\ell\left(\frac{1}{T}, \frac{Kp'}{K+1} + \frac{1}{A(K+1)}\right) - \ell\left(\frac{1}{T}, \frac{Kp'}{K+1} + \frac{1}{B(K+1)}\right) \right) \\ & \leq \frac{F}{2A(K+1)} \log 2 - \frac{F}{2B(K+1)} \log 2. \end{aligned} \quad (28)$$

By unfolding ℓ in the LHS and dividing both sides by F , the inequality (28) is rewritten as

$$\begin{aligned} & \frac{1}{2(K+1)} \left(\frac{1}{A} - \frac{1}{B} \right) \log 2 \geq \\ & \frac{1}{2T} \log\left(\frac{\frac{2}{T}}{\frac{1}{T} + \frac{Kp'}{K+1} + \frac{1}{A(K+1)}}\right) + \frac{1}{2} \left(\frac{Kp'}{K+1} + \frac{1}{A(K+1)} \right) \log\left(\frac{2\left(\frac{Kp'}{K+1} + \frac{1}{A(K+1)}\right)}{\frac{1}{T} + \frac{Kp'}{K+1} + \frac{1}{A(K+1)}}\right) \\ & - \frac{1}{2T} \log\left(\frac{\frac{2}{T}}{\frac{1}{T} + \frac{Kp'}{K+1} + \frac{1}{B(K+1)}}\right) - \frac{1}{2} \left(\frac{Kp'}{K+1} + \frac{1}{B(K+1)} \right) \log\left(\frac{2\left(\frac{Kp'}{K+1} + \frac{1}{B(K+1)}\right)}{\frac{1}{T} + \frac{Kp'}{K+1} + \frac{1}{B(K+1)}}\right) \\ & \equiv \frac{1}{(K+1)} \left(\frac{1}{A} - \frac{1}{B} \right) \log 2 - \frac{1}{(K+1)} \left(\frac{1}{A} - \frac{1}{B} \right) \log 2 \geq \\ & \frac{1}{T} \log\left(\frac{\frac{1}{T}}{\frac{1}{T} + P' + \frac{1}{A(K+1)}}\right) + \left(P' + \frac{1}{A(K+1)}\right) \log\left(\frac{P' + \frac{1}{A(K+1)}}{\frac{1}{T} + P' + \frac{1}{A(K+1)}}\right) \\ & - \frac{1}{T} \log\left(\frac{\frac{1}{T}}{\frac{1}{T} + P' + \frac{1}{B(K+1)}}\right) - \left(P' + \frac{1}{B(K+1)}\right) \log\left(\frac{P' + \frac{1}{B(K+1)}}{\frac{1}{T} + P' + \frac{1}{B(K+1)}}\right), \end{aligned}$$

where $P = \frac{Kp'}{K+1}$. Let $P_A = P' + \frac{1}{A(K+1)}$ and $P_B = P' + \frac{1}{B(K+1)}$, where $P_A \geq P_B$. Then, by cancelling out all identical terms, the above inequality is simplified as

$$\begin{aligned} & 0 \geq \frac{1}{T} \log\left(\frac{\frac{1}{T}}{\frac{1}{T} + P_A}\right) - \frac{1}{T} \log\left(\frac{\frac{1}{T}}{\frac{1}{T} + P_B}\right) \\ & + P_A \log\left(\frac{P_A}{\frac{1}{T} + P_A}\right) - P_B \log\left(\frac{P_B}{\frac{1}{T} + P_B}\right) \\ & \equiv 0 \geq \frac{1}{T} \log\left(\frac{\frac{1}{T} + P_B}{\frac{1}{T} + P_A}\right) + P_B \log\left(\frac{\frac{1}{T} + P_B}{P_B}\right) - P_A \log\left(\frac{\frac{1}{T} + P_A}{P_A}\right) \end{aligned}$$

If we multiply by T both sides, this inequality is implied by the two following inequalities:

$$\log\left(\frac{\frac{1}{T} + P_B}{\frac{1}{T} + P_A}\right) \leq 0, \quad (29)$$

$$\log\left(\frac{\left(1 + \frac{1}{TP_B}\right)^{TP_B}}{\left(1 + \frac{1}{TP_A}\right)^{TP_A}}\right) \leq 0. \quad (30)$$

The inequality (29) is trivial since $P_A \geq P_B$. For the inequality (30), the numerator and the denominator are in the form of $f(n) = \left(1 + \frac{1}{n}\right)^n$, which is a non-decreasing function. Thus, the denominator is always greater than or equal to the numerator, thus satisfying the inequality. \square

A.4 Proof of Corollary 1

Proof. Since HYPERREC measures a weighted average of the probabilistic distances that are defined for each head set node of the target arc, we consider each head set node $v_h \in H_i$ of the target arc e_i . Since the tail set size of every arc is identical to 1 (i.e., $|T_i| = 1$), there exists at most one arc in Ψ_i that covers a specific node v_h in the head set H_i of the target arc, i.e., $\forall v_h \in H_i$,

$$|\{e_k \in \Psi_i : v_h \in T_k\}| \leq 1, \quad (31)$$

Let v' be the target arc's tail set node, i.e., $T_i = \{v'\}$. Then, by the definition of Ψ_i , v' is included in the head set of every $e_k \in \Psi_i$, i.e., $\forall e_k \in \Psi_i$,

$$v' \in H_k. \quad (32)$$

Eq. (31) and Eq. (32) imply that, $\forall e_k \in R_i \subseteq \Psi_i$, Eq. (33) holds.

$$\text{JSD}(p_h \parallel p_h^*) = \ell(1, \frac{1}{|H_k|}) + \sum_{v \in H_k \setminus \{v'\}} \ell(0, \frac{1}{|H_k|}). \quad (33)$$

Let $A = |H_{k1}|$ and $B = |H_{k2}|$. Then, $\forall e'_{h1}, e'_{h2} \in R_i \subseteq \Psi_i$ s.t. $|H'_{h1}| \leq |H'_{h2}|$,

$$\begin{aligned} \text{JSD}(p_{h1} \parallel p_{h1}^*) &\leq \text{JSD}(p_{h2} \parallel p_{h2}^*) \\ &\equiv \ell(1, \frac{1}{|H_{k1}|}) + \sum_{v \in H_{k1} \setminus \{v'\}} \ell(0, \frac{1}{|H_{k1}|}) \leq \ell(1, \frac{1}{|H_{k2}|}) + \sum_{v \in H_{k2} \setminus \{v'\}} \ell(0, \frac{1}{|H_{k2}|}) \\ &\equiv \frac{1}{2A} \log(\frac{2}{1+A}) + \frac{1}{2} \log(\frac{2A}{1+A}) + \frac{A-1}{2A} \log 2 \\ &\leq \frac{1}{2B} \log(\frac{2}{1+B}) + \frac{1}{2} \log(\frac{2B}{1+B}) + \frac{B-1}{2B} \log 2 \\ &\equiv \log(\frac{A(B+1)}{B(A+1)}) + (\frac{1}{A} - \frac{1}{B}) \log 2 + \log((1+B)^{\frac{1}{B}}) - \log((1+A)^{\frac{1}{A}}) \leq (\frac{1}{A} - \frac{1}{B}) \log 2 \\ &\equiv \log(\frac{A(B+1)}{B(A+1)}) + \log(\frac{(1+B)^{\frac{1}{B}}}{(1+A)^{\frac{1}{A}}}) \leq 0, \end{aligned} \quad (35)$$

We prove the inequality (34) by showing that both first and second terms of the LHS of the inequality (35) are smaller than or equal to 0. Since $A \leq B$, it is trivial that the first term is smaller than or equal to 0. The second term has a functional form of $\log(f(x)/f(x'))$ where $f(x)$ is a non-increasing function and $x \leq x'$, and thus the second term is also smaller than or equal to 0.

In addition, let $e'_h \in \Psi_i$ be the only arc where $T'_h = \{v_h\}$. Then, the probabilistic distance at a each head set node v_h depends on whether e'_h is in any reciprocal set $R_i \subseteq \Psi_i$ as follows:

$$\mathcal{L}(p_h, p_h^*) = \begin{cases} \text{JSD}(p'_h \parallel p_h^*) & \text{if } e'_h \in R_i \\ \mathcal{L}_{max} & \text{otherwise,} \end{cases} \quad (36)$$

where p'_h is the probability distribution at v_h when the reciprocal set $R_i = \{e'_h\}$, p_h^* is the optimal probability distribution at a node $v_h \in H_i$.

By Eq. (31) and Eq. (36), for any $R'_i = \{e'_{h1}, \dots, e'_{hk}\} \subseteq \Psi_i$, Eq. (37) holds.

$$r(e_i, R'_i) = \left(\frac{1}{k}\right)^\alpha \left(1 - \frac{\text{JSD}(p'_{h1} \parallel p_{h1}^*) + \dots + \text{JSD}(p'_{hk} \parallel p_{hk}^*) + (|H_i| - k) \times \mathcal{L}_{max}}{|H_i| \times \mathcal{L}_{max}}\right), \quad (37)$$

where $T'_{hj} = \{v_{hj}\}$ for every $j \in \{1, \dots, k\}$. In addition, Eq. (37) and the inequality (34) imply that drawing k reciprocal arcs from Ψ_i in ascending order of their head set size achieves the maximum reciprocity for fixed k . Let $\Gamma_{i,k}$ be such a reciprocal set. Formally, if we let $\Gamma_{i,k}$ be a subset of Ψ_i such that $|\Gamma_{i,k}| = k$ and $|H_s| \leq |H_t|$, $\forall e_s \in \Gamma_{i,k}$, $\forall e_t \in \{\Psi_i \setminus \Gamma_{i,k}\}$, then $\arg\max_{R_i \subseteq \Psi_i \text{ s.t. } |R_i|=k} r(e_i, R_i) = \Gamma_{i,k}$ holds. \square

B Appendix: Limitations of Baseline Measures

In this section, we show why several baseline measures fail in satisfying some of **Axiom 1-8**. Below, We use $G_i = (V_i, E_i)$ and $G_j = (V_j, E_j)$ to denote the hypergraphs on the left side and the right side, respectively, of each subfigure of Figure 2.

Table 10: Violation of **Axiom 3**. We use G_i and G_j to denote the hypergraphs on the left side and the right side, respectively, of each subfigure of Figure 2. This table reports the computed reciprocity values, $r(G_i)$ and $r(G_j)$, of [Pearcy et al., 2014] (B1), and the computed reciprocity values, $r(e_i, R_i)$ and $r(e_j, R_j)$, of the ratio of covered pairs (B2) and HYPERREC without size penalty (B5), for Figures 2(d)-(e). In order to satisfy **Axiom 3**, $r(e_i, R_i) < r(e_j, R_j)$ (or $r(G_i) < r(G_j)$) should hold in both subfigures. Note that, B1, B2, and B5 cannot satisfy the inequality in at least one subfigure.

	Figure 2(d) (Axiom 3A)		Figure 2(e) (Axiom 3B)	
	$r(e_i, R_i)$ or $r(G_i)$	$r(e_j, R_j)$ or $r(G_j)$	$r(e_i, R_i)$ or $r(G_i)$	$r(e_j, R_j)$ or $r(G_j)$
B1 (Pearcy et al. [2014])	0.2093	0.2093	0.2093	0.2093
B2 (Ratio of Covered Pairs)	0.5625	0.5625	0.5625	0.5625
B5 (HYPERREC w/o Size Penalty)	0.6333	0.6446	0.6446	0.6446

Table 11: Violation of **Axiom 4**. The computed reciprocity values, $r(e_i, R_i)$ and $r(e_j, R_j)$, of the ratio of covered pairs (B2) and the penalized ratio of covered pairs (B3) with $\alpha = 1$ in Figure 2(f). While $r(e_i, R_i) < r(e_j, R_j)$ should hold to satisfy **Axiom 4**, the inequality does not hold for B2 and B3.

	Figure 2(f) (Axiom 4)	
	$r(e_i, R_i)$	$r(e_j, R_j)$
B2 (Ratio of Covered Pairs)	1.00	1.00
B2 (Penalized Ratio of Covered Pairs)	0.25	0.25

B.1 Violations of Axiom 3

We show how several baseline measures violate **Axiom 3**. In Figures 2(d)-(e), $r(e_i, R_i) < r(e_j, R_j)$ should hold in order to satisfy **Axiom 3**. However, we numerically verify that $r(e_i, R_i) = r(e_j, R_j)$ hold for some baseline measures, which violates **Axiom 3**.

B1. [Pearcy et al., 2014]: They use clique expansion, which transforms every hyperedge of a hypergraph to a clique of a pairwise graph (e.g., $\langle\{v_1\}, \{v_2, v_3\}\rangle \rightarrow \{\langle\{v_1\}, \{v_2\}\rangle, \langle\{v_1\}, \{v_3\}\rangle\}$). Through this process, the original hypergraph is transformed into a weighted digraph (see Section 2.2). Since Pearcy et al. [2014] do not propose any arc-level reciprocity, we compare its hypergraph-level reciprocity for counterexamples regarding **Axiom 3**. That is, we compare $r(G_i)$ and $r(G_j)$ in Figures 2(d)-(e). As reported in Table 10, $r(G_i) = r(G_j) = 0.2093$ and $r(G_i) = r(G_j) = 0.2093$ hold in Figure 2(d) and Figure 2(e), respectively, violating **Axiom 3**.

B2. Ratio of Covered Pairs: We compare the ratio of covered pairs (B2), which is arc-level reciprocity, in Figures 2(d)-(e). As reported in Table 10, $r(e_i, R_i = \{e'_{i1}, e'_{i2}\}) = r(e_j, R_j = \{e'_j\}) = 0.5625$ and $r(e_i, R_i) = r(e_j, R_j) = 0.5625$ hold in Figure 2(d) in Figure 2(e), respectively, which violates **Axiom 3**.

B5. HyperRec w/o Size Penalty: As reported in Table 10, $r(e_i, R_i = \{e'_{i1}, e'_{i2}\}) = r(e_j, R_j = \{e'_j\}) = 0.6446$ holds in Figure 2(e), which violates **Axiom 3**.

B.2 Violations of Axiom 4

We show how several baseline measures violate **Axiom 4**. In Figure 2(f), $r(e_i, R_i) < r(e_j, R_j)$ should hold in order to satisfy **Axiom 4**. However, we numerically verify that $r(e_i, R_i) = r(e_j, R_j)$ hold for some baseline measures, which violates **Axiom 4**.

B2. Ratio of Covered Pairs: As reported in Table 11, $r(e_i, R_i = (E_i \setminus \{e_i\})) = r(e_j, R_j = E_j \setminus \{e_j\}) = 1.00$ holds in Figure 2(f), which violates **Axiom 4**.

B3. Penalized Ratio of Covered Pairs: As reported in Table 11, $r(e_i, R_i = (E_i \setminus \{e_i\})) = r(e_j, R_j = E_j \setminus \{e_j\}) = 0.25$ holds in Figure 2(f), which violates **Axiom 4**.

B.3 Violations of Axiom 5

B4. HyperRec w/o Normalization: In order to satisfy **Axiom 5**, reciprocity should always lie in a fixed finite range. Here, we demonstrate that (B4) violates **Axiom 5** by showing that its reciprocity value can become infinite. Recall that (B4) is defined as

$$r(e_i, R_i) = \left(\frac{1}{|R_i|} \right)^\alpha \left(|H_i| - \frac{\sum_{v_h \in H_i} \mathcal{L}(p_h, p_h^*)}{\mathcal{L}_{max}} \right). \quad (38)$$

Consider a case where $R_i = \{e'_i = \langle T_i, H_i \rangle\}$. Then, for each $v_h \in H_i$, $\mathcal{L}(p_h, p_h^*) = 0$ holds. In turn, Eq (38) becomes $r(e_i, R_i) = |H_i|$. In this case, as $|H_i|$ approaches infinity, $r(e_i, R_i)$ also becomes infinite. Since the value of (B4) does not lie in a fixed finite range, (B4) violates **Axiom 5**.

B.4 Violations of Axiom 6

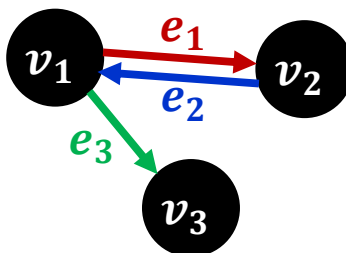


Figure 8: A counterexample that shows that some baseline measures fail to satisfy **Axiom 6**.

B1. [Pearcy et al., 2014]: Consider the digraph in Figure 8. The digraph reciprocity of the digraph is $r(G) = \frac{2}{3}$ since $E = \{e_1, e_2, e_3\}$, and $E^{\leftrightarrow} = \{e_1, e_2\}$. In this case, however, the clique-expanded adjacency matrices of the digraph and the perfectly reciprocal hypergraph are

$$\bar{A} = \begin{pmatrix} 0 & 1 & 1 \\ 1 & 0 & 0 \\ 0 & 0 & 0 \end{pmatrix} \text{ and } \bar{A}' = \begin{pmatrix} 0 & 1 & 1 \\ 1 & 0 & 0 \\ 1 & 0 & 0 \end{pmatrix}.$$

Thus, according to the definition in [Pearcy et al., 2014], the reciprocity becomes $\frac{2}{4} = 0.5$ because $tr(\bar{A}^2) = 2$ and $tr(\bar{A}'^2) = 4$. Since $\frac{2}{4} \neq \frac{2}{3}$, [Pearcy et al., 2014] (B1) violates **Axiom 6**.

B6. HyperRec with All Arcs as Reciprocal Set: According to **Axiom 6**, a hypergraph reciprocity value should equal $2/3 \approx 0.6667$ in Figure 8. If we let $\alpha = 1$, then the overall hypergraph-level reciprocity ($r(G)$) based on HYPERREC with all arcs as the reciprocal set (B6) is

$$\begin{aligned} r(e_1, \{e_2, e_3\}) &= 0.5, \quad r(e_2, \{e_1, e_3\}) = 0.3444, \quad \text{and} \quad r(e_3, \{e_1, e_2\}) = 0 \\ r(G) &= \frac{r(e_1, \{e_2, e_3\}) + r(e_2, \{e_1, e_3\}) + r(e_3, \{e_1, e_2\})}{3} \\ &= \frac{0.5 + 0.3444 + 0}{3} = 0.2815 \neq 0.6667 \end{aligned}$$

which violates **Axiom 6**.

B.5 Violations of Axiom 8

B6. HyperRec with All the Arcs as Reciprocal Set: Even when there exists the perfect reciprocal opponent of a specific arc, the transition probability cannot be identical to the optimal transition probability if there exists another inversely overlapping arc (see the target arc e_2 's case in Figure 8).

B7. HyperRec with Inversely Overlapping Arcs as Reciprocal Set: As in the previous case, if there exist multiple inversely overlapping arcs, all of them are included in the reciprocal set. As a result, for such arcs, the cardinality penalty term gets smaller than 1 (i.e., $(1/|R_i|)^\alpha < 1$), resulting in $r(e_i, R_i) < 1$. Consequently, the overall hypergraph reciprocity becomes smaller than 1.

C Appendix: Data Description

In this section, we provide the sources of the considered datasets and describe how we preprocess them.

Metabolic datasets: We use two metabolic hypergraphs, **iAF1260b** and **iJO1366**, which are provided by [Yadati et al., 2020]. They are provided in the form of directed hypergraphs, and they do not require any pre-processing. We remove one hyperarc from each dataset since their head set or tail set is abnormally large. Specifically, the size of their head sets is greater than 20, while the second largest one is 8. Each node corresponds to a gene, and each hyperarc indicates a metabolic reaction among them. Specifically, a hyperarc e_i indicates that a reaction among the genes in the tail set T_i results in the genes in the head set H_i .

Email datasets: We use two email hypergraphs, **email-enron** and **email-eu**. The **Email-enron** dataset is provided by [Chodrow and Mellor, 2020]. We consider each email as a single hyperarc. Specifically, the head set is composed of the receiver(s) and cc-ed user(s), and the tail set is composed of the sender. The **Email-eu** dataset is from SNAP [Leskovec and Krevl, 2014]. The original dataset is a dynamic graph where each temporal edge from a node u to a node v at time t indicates that u sent an email to v at time t . The edges with the same source node and timestamp are replaced by a hyperarc, where the tail set consists only of the source node and the head set is the set of destination nodes of the edges. Note that every hyperarc in these datasets has a unit tail set, i.e., $|T_i| = 1, \forall i = \{1, \dots, |E|\}$.

Citation datasets: We use two citation hypergraphs, **citation-data mining** and **citation-software**, which we create from pairwise citation networks, as suggested by [Yadati et al., 2021]. Nodes are the authors of publications. Assume that a paper A , which is co-authored by $\{v_1, v_2, v_3\}$, cited another paper B , which is co-authored by $\{v_4, v_5\}$. Then, this citation leads to a hyperarc where the head set is $\{v_4, v_5\}$ and the tail set is $\{v_1, v_2, v_3\}$. As pairwise citation networks, we use subsets of a DBLP citation dataset [Sinha et al., 2015]. The subsets consist of papers published in the venues of data mining and software engineering, respectively.⁷ In addition, we filter out all papers co-authored by more than 10 authors to minimize the impact of such outliers.

Question answering datasets: We use two question answering hypergraphs, **qna-math** and **qna-server**. We create directed hypergraphs from the log data of a question answering site, *stack exchange*, provided at [Archive, 2022]. Among various domains, we choose *math-overflow*, which covers mathematical questions, and *server-fault*, which treats server related issues. The original log data contains the posts of the site, and one questioner and one or more answerers are involved with each post. We ignore all posts without any answerer. We treat each user as a node, and we treat each post as a hyperarc. For each hyperarc, the questioner of the corresponding post composes the head set, and the answerer(s) compose the tail set. Note that every hyperarc in these datasets has a unit head set, i.e., $|H_i| = 1, \forall i = \{1, \dots, |E|\}$.

Bitcoin transaction dataset: We use three bitcoin transaction hypergraphs, **bitcoin-2014**, **bitcoin-2015**, and **bitcoin-2016**. The original datasets are provided by [Wu et al., 2021], and they contain first 1,500,000 transactions in 11/2014, 06/2015, and 01/2016, respectively. We model each account as a node, and we model each transaction as a hyperarc. As multiple accounts can be involved in a single transaction, the accounts from which the coins are sent compose the tail set, and the accounts to which the coins sent compose the head set. We remove all transactions where the head set and the tail set are exactly the same.

⁷We use the venues listed at [Wikipedia, 2022]